



# Intranasal vaccination with probiotic *Escherichia coli* membrane vesicles displaying pneumococcal capsular polysaccharides elicits mucosal immunity



Ryoma Nakao <sup>1</sup>✉, Soichiro Kimura<sup>2,3</sup>, Kimihiro Abe<sup>1,4</sup>, Takehiro Yamaguchi<sup>1</sup>, Eisuke Kuroda<sup>5,6,7</sup>, Shigeto Hamaguchi<sup>5,7</sup>, Kazuhiro Tateda<sup>3</sup>, Yukino Ohki<sup>8</sup>, Naoki Narisawa<sup>8</sup>, Makoto Ohnishi<sup>1</sup> & Yukihiko Akeda<sup>1</sup>

A novel vaccine modality is needed to generate both systemic and mucosal immunity in the respiratory tract, where pathogens are most likely to colonize and to initiate infection. Here, we demonstrated that intranasal immunization with probiotic *Escherichia coli*-derived membrane vesicles displaying serotype-14 pneumococcal capsule (CPS14<sup>+</sup>MVs) elicited potent IgG responses without adjuvant in mice, which were comparable and significantly superior to those of the injected CPS14<sup>+</sup>MVs and two licensed pneumococcal vaccines (conjugate and polysaccharide types), respectively. Notably, IgA class-switch recombination occurred only with intranasal CPS14<sup>+</sup>MVs immunization, resulting in robust secretory IgA (SIgA) production throughout a one-year-long-term study. Furthermore, the intranasal CPS14<sup>+</sup>MV vaccine induced both systemic and mucosal immunity regardless of mouse age at vaccination. Whereas opsonophagocytic activities were detected in sera of all immunization groups, only the intranasal CPS14<sup>+</sup>MV vaccine achieved dramatic pneumococcal clearance in the nasal cavity. Nevertheless, it failed to protect isogenic *pIgR*<sup>-/-</sup> mice, which are genetically impaired for SIgA translocation, from colonization of the respiratory tract. In conclusion, the present study could offer a novel vaccination strategy using chimeric probiotic *E. coli* MVs to provide antibody-mediated protection against pneumococcal colonization and infection.

*Streptococcus pneumoniae* (pneumococcus) is one of the leading causes of respiratory tract infection, not only in children<sup>1</sup>, but also in adults<sup>2,3</sup>. As a species, over 100 antigenically and biochemically unique capsular polysaccharide CPS types (serotypes) have been reported to date<sup>4-6</sup>. Since the 2000s, the introduction of current pneumococcal vaccines, which target the most common disease-associated serotypes, has contributed to a reduction in the global burden of invasive pneumococcal disease (IPD)<sup>1,7</sup>. However, pneumococcal vaccines also led to immunological escape of certain *S.*

*pneumoniae* serotypes and replacement by serotypes not recognized by the vaccines. Replacement by non-vaccine serotypes has been a major concern in clinical settings<sup>8-10</sup>. Moreover, pneumococcal resistance to antimicrobials is a serious and rapidly increasing problem<sup>11-13</sup>. Therefore, development of a novel pneumococcal vaccine that outperforms current vaccine strategies remains a high priority.

Two types of pneumococcal vaccines currently approved are the polyvalent pneumococcal polysaccharide vaccine (PPSV) and the polyvalent

<sup>1</sup>Department of Bacteriology I, National Institute of Infectious Diseases, Japan Institute for Health Security (JIHS), Shinjuku-ku, Tokyo, Japan. <sup>2</sup>Division of Infection Prevention and Control, Faculty of Pharmaceutical Sciences, Shonan University of Medical Sciences, Yokohama, Kanagawa, Japan. <sup>3</sup>Department of Microbiology and Infectious Diseases, Faculty of Medicine, Toho University School of Medicine, Ota-ku, Tokyo, Japan. <sup>4</sup>Research Center for Vaccine Development, National Institute of Infectious Diseases, Japan Institute for Health Security (JIHS), Shinjuku-ku, Tokyo, Japan. <sup>5</sup>Department of Transformative Analysis for Human Specimen, Osaka University Graduate School of Medicine, Suita, Osaka, Japan. <sup>6</sup>Division of Fostering Required Medical Human Resources, Center for Infectious Disease Education and Research (CiDER), Osaka University, Suita, Osaka, Japan. <sup>7</sup>Division of Infection Control and Prevention, Osaka University Hospital, Suita, Osaka, Japan. <sup>8</sup>Department of Food Bioscience and Biotechnology, College of Bioresource Science, Nihon University; 1866, Kameino, Fujisawa, Kanagawa, Japan. ✉e-mail: [nakao.ry@jihs.go.jp](mailto:nakao.ry@jihs.go.jp)

pneumococcal conjugate vaccines (PCVs). Both PPSV and PCVs target the limited number of CPS serotypes that frequently cause IPD, and are effective in reducing disease severity and preventing hospitalization after infection by the vaccine serotypes. PPSV23 covers more serotypes than PCVs, while the antibody responses are weaker than those elicited by PCVs, as pneumococcal polysaccharides are T-cell-independent antigens. On the other hand, PCVs contained different CPS types conjugated to a protein carrier CPM197 and absorbed on aluminum phosphate to enhance T-cell-dependent immunity. PCVs have been sequentially developed in recent years to cover wider pneumococcal serotypes, i.e., the prototype PCV7 to more polyvalent ones: PCV13, PCV15, PCV20, and PCV21<sup>14</sup>. On the other hand, as the polysaccharides are per se T-cell-independent antigens, insufficient immunogenicity not only of PPSV but also of PCVs has been described<sup>15</sup>. The cost-effectiveness of PCVs is also controversial<sup>16</sup>.

As with most vaccines currently in use for respiratory tract infections, PPSV and PCVs are both injected vaccines, which are inferior to mucosal vaccines in that they will not elicit nasopharyngeal secretory IgA (SIgA) responses. On the other hand, mucosal vaccines, such as intranasal vaccines, elicit mucosal immune responses through activating the immune system at mucosal-associated lymphoid tissues (MALT), followed by enhanced SIgA responses, which may efficiently block pathogen entry at the epithelium. In fact, intranasal vaccines against the influenza virus and SARS-CoV-2 have been approved for use in humans<sup>17-21</sup>. Together, intranasal vaccines might protect from pneumococcal disease more efficiently than injected vaccines. However, regarding pneumococcal vaccines, there are few reports from in vivo studies, especially assessing vaccination route or comparing efficacy with licensed vaccines. In addition, it is unclear how well SIgA will protect from pneumococci in the nasopharynx.

Membrane vesicles (MVs) are nanometer-sized exosomes derived from bacteria. MVs are potentially effective vaccine vehicles for infectious diseases because they can carry a wide range of immunomodulators to be displayed on or packaged within the stable nanoparticles. Recently, we reported a breakthrough biotechnology technique called the “glycine induction method” for MV production from a probiotic *Escherichia coli* (EcN) strain<sup>22,23</sup>. Utilizing this method, a large quantity of MVs with low endotoxin content can be isolated very efficiently<sup>22,23</sup>, which may help shape future manufacturing of MV-based vaccines. Furthermore, we have characterized serotype-14 pneumococcal CPS-expressing MVs (CPS14<sup>+</sup>MVs), which are isolated from the culture supernatant of a genetically modified probiotic *Escherichia coli* (EcN) clone<sup>24</sup> using the glycine induction method<sup>22,23</sup>. Durable and potent immunomodulatory capacity of CPS14<sup>+</sup>MVs was observed when the vaccine was administered parenterally in vivo<sup>24</sup>. However, how long and to what extent intranasal immunization with CPS14<sup>+</sup>MVs elicits systemic and mucosal immune responses, and whether intranasal CPS14<sup>+</sup>MVs vaccine prevents colonization in the respiratory tract, remains unknown.

In the present study, our findings highlight for the first time a promising intranasal vaccine platform based on MVs targeting pneumococcal CPS, which achieved persistent antibodies not only in the bloodstream, but also in the respiratory tracts for over one year. Moreover, the nasal CPS14<sup>+</sup>MV vaccine had clear advantages over the injected vaccine as well as compared to two current licensed vaccines in the context of protection from pneumococci, i.e., offering antibody-mediated protection against both pneumococcal colonization and infection. Here, we discuss the general applicability of the present MV-based vaccine platform for infectious diseases by not only other serotypes of pneumococcus, but also other encapsulated bacterial pathogens that initiate infection at the mucosa.

## Results

### Nasal CPS14<sup>+</sup>MV vaccine is highly immunogenic without adjuvant

Recently, we characterized flagellar-deficient probiotic *E. coli* (EcNΔ*flihD*)-derived MVs displaying serotype-14 pneumococcal CPS (CPS14<sup>+</sup>MVs) at high density, which elicited a potent IgG response when administered by injection to mice<sup>24</sup>. To further expand the applicability of CPS14<sup>+</sup>MVs for

intranasal vaccines, we first examined whether and how CPS14<sup>+</sup>MVs elicit mucosal immune responses by a standard intranasal vaccination regimen (Fig. 1A). In the control arms, mice were intranasally immunized with purified CPS14. CPS14 was also co-administered with poly (I:C), cholera toxin B (CTB), or EcNΔ*flihD* MVs. Poly (I:C) and CTB were chosen as authentic nucleic acid-based and toxin-based mucosal adjuvants, respectively. EcNΔ*flihD* MVs were chosen because they function as a robust mucosal adjuvant when ovalbumen was used as a model protein antigen<sup>23</sup>. To define their adjuvanticities towards polysaccharide antigen CPS14, CPS14-specific antibodies in mice after immunization were measured by ELISA (Fig. 1B). The results showed that intranasal immunization with purified CPS14 alone or CPS14 plus different adjuvants induced only a weak IgM response, but neither IgG nor IgA was produced in the blood (Fig. 1B). As with the case of intranasal immunization with CPS14 alone or CPS plus different adjuvants (Fig. 1), intranasal immunization with a licensed conjugate “parenteral” vaccine PCV13 elicited only weak IgM in blood (data not shown). In contrast, intranasal CPS14<sup>+</sup>MV vaccines elicited serum IgG and IgA responses, as well as IgA responses in the samples of eye wash, saliva, nasal wash, and brochoalveolar lavage fluid (BALF) (Fig. 1). Intranasal immunization with different amounts of CPS14<sup>+</sup>MVs revealed that serum IgG responses were elicited in a dose-dependent manner (Fig. S1), and there was a trend of dose-dependency on IgA responses in the samples of serum, saliva, nasal wash, BALF, and feces (Fig. S1). On the other hand, there was a trend of declining IgA responses in serum, saliva, BALF, and feces samples when the dose of CPS14<sup>+</sup>MVs increased to 10 µg (Fig. S1). Therefore, intranasal CPS14<sup>+</sup>MV vaccines at a dose of 1 µg elicited robust production of not only serum IgG, but also IgA in the serum, saliva, nasal cavities, lung, and feces (Fig. S1). Serum IgE was not detected in any of the mice, irrespective of the vaccine types used (Figs. 1 and S1). The series of experiments using our intranasal mouse model suggests that mucosal immunogenicity towards CPS14 was achieved only when the CPS14 moieties were displayed on the MVs.

### Long-term follow-up of mice after intranasal immunization with CPS14<sup>+</sup>MVs

Next, we examined whether the intranasal CPS14<sup>+</sup>MV vaccine could confer long-term mucosal immunity. The grouping and timeline of the long-term experiment are shown in Fig. 2A and B, respectively. The CPS14-specific immune responses in blood and saliva over time were measured by ELISA (Fig. 3). The intranasal CPS14<sup>+</sup>MV vaccine group was named Grp. B. As controls, mice were intranasally immunized with MVs isolated from the control EcNΔ*flihD* strain that harbors an empty vector (Grp. A), and mice were also subcutaneously immunized with CPS14<sup>+</sup>MVs (Grp. C), PCV13 (Grp. D), PPSV23 (Grp. E), and PBS (Grp. F). Although the results of Grps. C-F have been previously published<sup>24</sup>, they were re-analyzed to compare the immunogenicity of the intranasal CPS14<sup>+</sup>MV vaccine (Grp. B) with those of the injected CPS14<sup>+</sup>MV vaccine (Grp. C) and two current pneumococcal vaccines (Grps. D and E). The intranasal CPS14<sup>+</sup>MV vaccine (Grp. B) elicited a potent IgG response in blood for over one year (Fig. 3). The strength and durability of IgG production in the intranasal CPS14<sup>+</sup>MV vaccine (Grp. B) were comparable to those of the injected CPS14<sup>+</sup>MV vaccine (Grp. C), and were superior to those of PCV13 (Grp. D) and PPSV23 (Grp. E) (Fig. 3). Of note, the intranasal CPS14<sup>+</sup>MV vaccine (Grp. B) was the only one that could also elicit IgA class-switch recombination (CSR), and strong IgA responses were observed in both the blood and oral cavity during the one-year timeframe (Fig. 3). No IgE was detected in any of the mice used in this study (data not shown).

At the end of the long-term study, the upper respiratory tract infection with serotype 14 pneumococci was performed to examine bacterial clearance activity in nasal cavity at 14 or 15 months after the 1st immunization, as shown in the timeline (Fig. 2B). All the aged mice were euthanized one day after the infection experiment, and samples of whole blood, BALF, and nasal wash were collected from infected mice, and the amount of CPS14-specific antibodies were examined (Fig. 4). In both injected and intranasal CPS14<sup>+</sup>MV vaccines (Grps. B and C), potent IgG

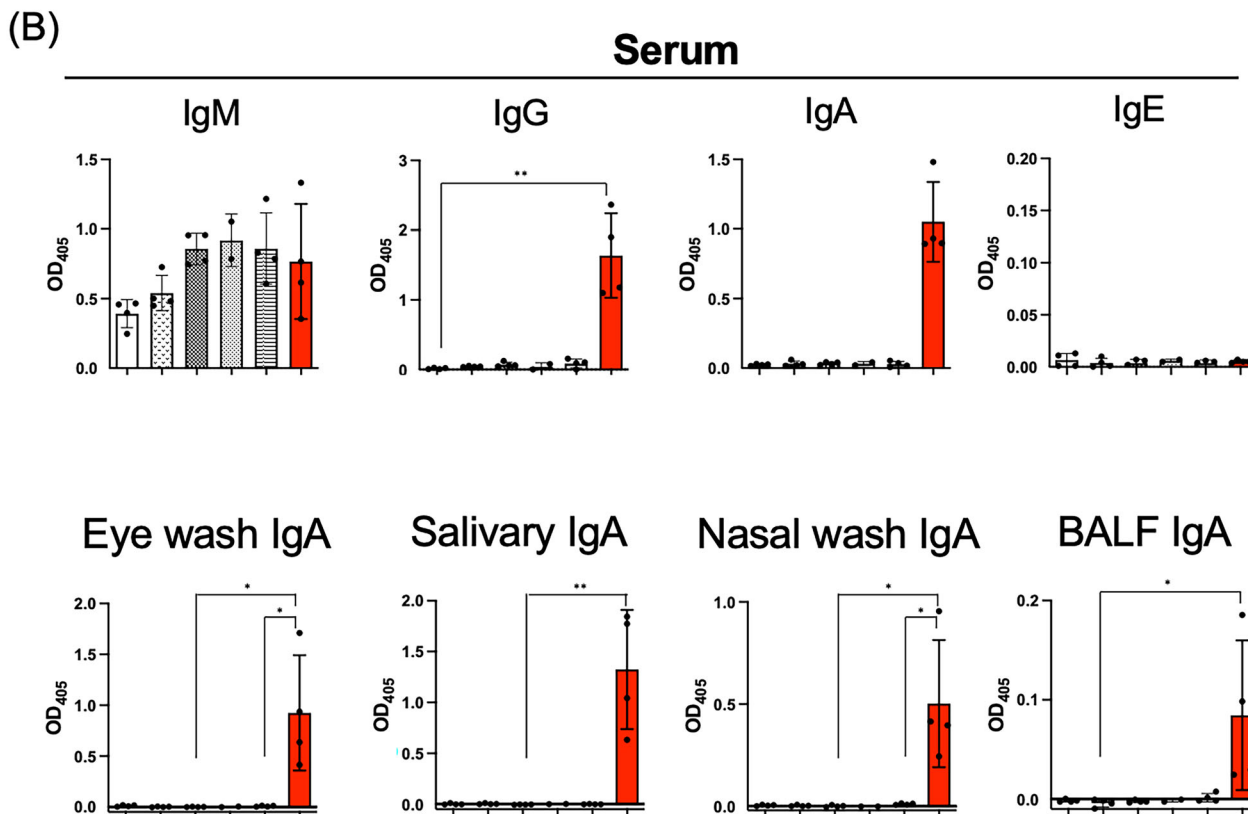
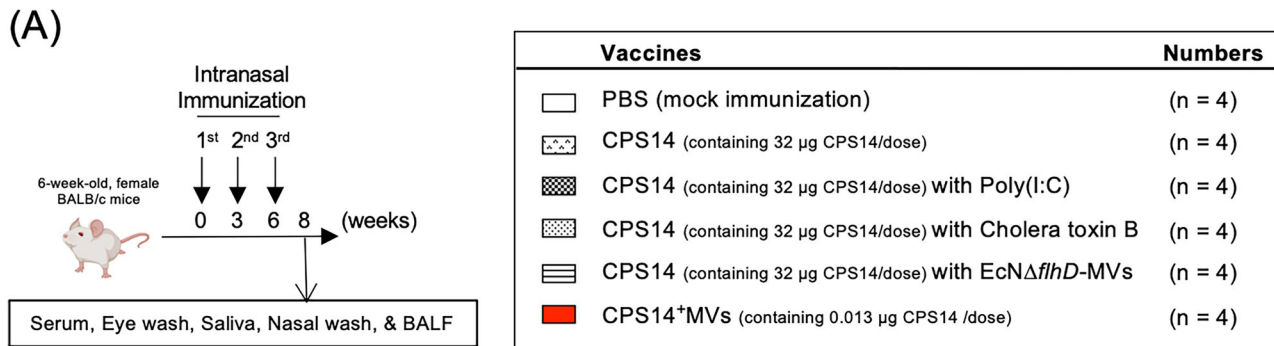


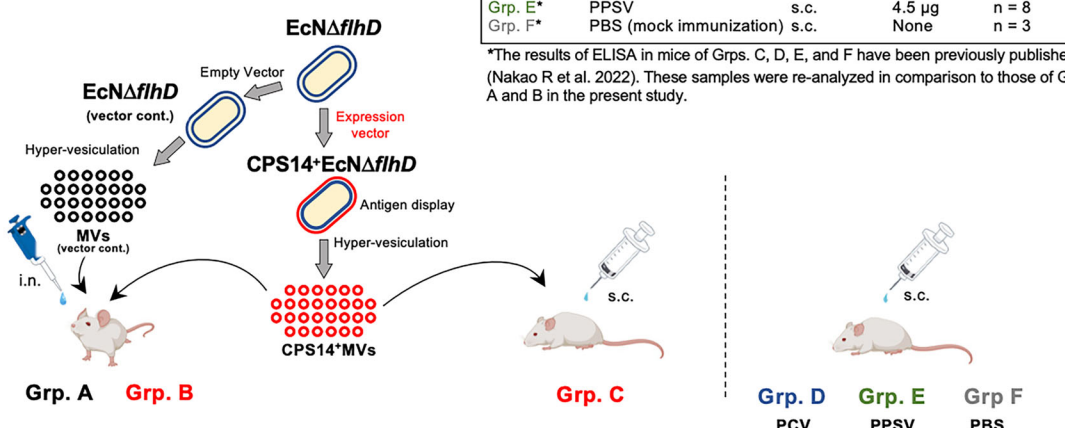
**Fig. 1 | Advantage of CPS14<sup>+</sup>MV vaccine over conventional polysaccharide vaccine when administered intranasally.** A Timeline of intranasal immunization and sample collection. Six-week-old female BALB/c mice ( $n = 24$ ) were equally distributed into six groups and intranasally immunized with PBS, CPS14 (32 µg) alone, CPS14 (32 µg) with Poly (I:C) (5 µg), CPS14 (32 µg) with cholera toxin B (10 µg), CPS14 (32 µg) with flagella-deficient probiotic *E. coli* (EcNΔflhD) MVs (1 µg as protein equivalent), and CPS14<sup>+</sup>MVs (1 µg as protein equivalent), three times at weeks 0, 3, and 6. Serum, eye wash, saliva, nasal wash, and BALF samples were collected at week 8. The amount of CPS14 in CPS14<sup>+</sup>MVs (1 µg) was estimated to be 0.013 µg. Vaccination groupings of mice are described in the box table in the upper right, which shows the used vaccine, the route, the amount of CPS14 per dose, and the number of mice in each group. Created in BioRender. Konig, S. (2025) <https://BioRender.com/z8u1cwz>.

**B** CPS14 ELISA. CPS14-specific antibodies in serum, eye wash, saliva, nasal wash, and BALF samples were measured by ELISA. In all ELISA except for serum IgG, samples were measured at 1:100 dilution. In ELISA for serum IgG, the samples were used at 1:1000 dilution. The results of all ELISA except for serum IgM and serum IgG are expressed as OD<sub>405</sub> values (mean  $\pm$  SD) after a 120-min incubation with AP substrate. The results of IgM and IgG ELISA are expressed as OD<sub>405</sub> values (mean  $\pm$  SD) after a 60-min incubation with AP substrate. The number of mice analyzed was four in all groups except the group of “CPS14 with Cholera toxin B”. The number of mice in the group of “CPS14 with Cholera toxin B” was 2, due to the accidental deaths of 2 mice in the group. Shown are the results of the statistical analysis using the Kruskal-Wallis test. \* $p < 0.05$ . \*\* $p < 0.01$ . Representative data were obtained from the 24 mice in one independent animal experiment.

production was detected. Furthermore, only the intranasal CPS14<sup>+</sup>MV vaccine elicited a dramatic IgA CSR (Fig. 4A) and robust CPS14-specific IgA responses were observed not only in the blood, but also in the nasal cavity and lung (Fig. 4A). IgG subclass analysis (Fig. 4B and C) revealed that both the intranasal and injected CPS14<sup>+</sup>MV vaccines elicited balanced IgG subclasses, while PCV13 elicited a strong Th2-type immune response biased toward IgG1 (Fig. 4B and C), which is consistent with our previous report<sup>24</sup>. When comparing the intranasal and

injected CPS14<sup>+</sup>MV vaccines, the level of BALF IgG2b in the intranasal CPS14<sup>+</sup>MV vaccine (Grp. B) was significantly higher than that in the injected CPS14<sup>+</sup>MV vaccine (Grp. C) (Fig. 4B). In contrast, the serum IgG1 level of the injected CPS14<sup>+</sup>MV vaccine (Grp. C) was significantly higher than that of the intranasal CPS14<sup>+</sup>MV vaccine (Grp. B) (Fig. 4B and C). On the other hand, IgG2a level was comparable between Grps. B and C (Fig. 4B and C), and there was no significant difference in the Th1/Th2 ratio between the two groups (Fig. 4C).

(A)



(B)

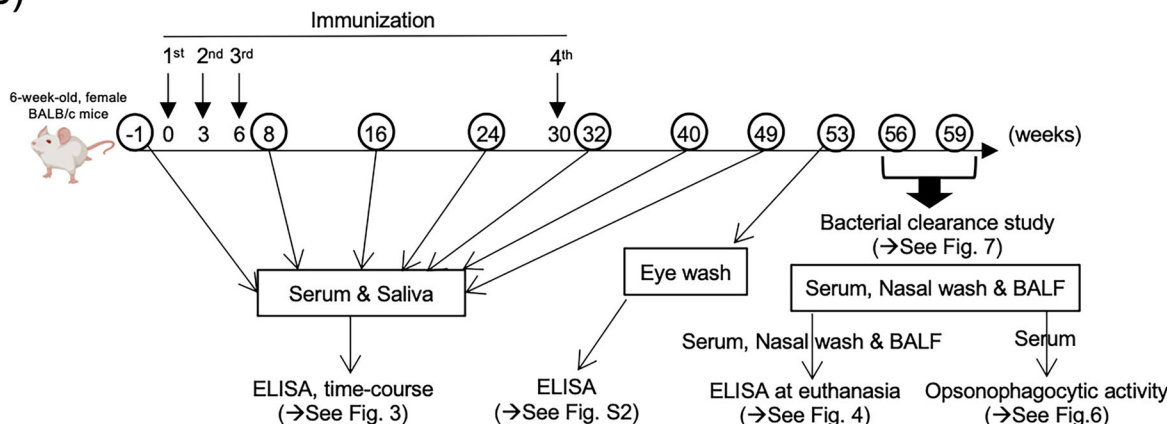


**Fig. 2 | Long-term animal study overview.** A Schematic representation of the types of vaccines and routes used in this study. Six-week-old female BALB/c mice ( $n = 43$ ) were grouped into six different regimens. The number of mice in all groups except Grp. F was 8. The number of mice in Grp. F was 3. Vaccination groupings of mice are described in the box table in the upper right, which shows the vaccine used, the route, the amount of CPS14 per dose, and the number of mice in each group. Grps. A and B mice were intranasally immunized with MVs (vector control) and CPS14+MVs, respectively. The results of ELISA in mice of Grps C–F have been previously published<sup>24</sup>. These samples were re-analyzed in comparison to those of Grps A (MVs, i.n.) and B (CPS14+MVs, i.n.) in the present study. The experiment including i.n. groups (Grps A and B) was performed at the same moment as the previously published experiment, including s.c. groups (Grps C–F)<sup>24</sup>. Representative data of the long-term animal study were obtained from the 43 mice in one independent animal experiment. Created in BioRender. Konig, S. (2025) <https://BioRender.com/z8u1cwz>. B Timeline of vaccine regimen, sample collection, and challenge with pneumococci. As shown in

Fig. 2A, BALB/c mice were intranasally immunized with MVs (vector control) and CPS14+MVs, and subcutaneously immunized with three different vaccines (CPS14+MVs, PCV, and PPSV) and PBS four times (at weeks 0, 3, 6, and 30). Serum and saliva samples were collected from the mice at seven different time points (weeks -1, 8, 16, 24, 32, 40, and 49). See the time-course data of ELISA at the seven different time points in Fig. 3. Eye wash was collected at week 53. See the data of ELISA using eye wash samples at week 53 in Fig. S2. All mice that survived until the end of the long-term animal experiment were subjected to the upper respiratory tract infection assay at week 56 or 59 ( $n = 40$ ). The mice ( $n = 40$ ) were divided into Class I ( $n = 18$ ) and Class II ( $n = 20$ ), which were assayed at weeks 56 and 59, respectively. See details of the grouping and randomization of mice in the “Materials and methods” section. See the bacterial clearance assay results in Fig. 7. Whole blood, nasal wash, and BALF were obtained after the bacterial clearance assay. See the results of ELISA and opsonophagocytic killing assays using the samples from mice at euthanasia in Figs. 4 and 6, respectively. Created in BioRender. Konig, S. (2025) <https://BioRender.com/z8u1cwz>.

### Declined antigenicity of MVs by displaying CPS14

To examine whether CPS14+MV vaccines also elicit antibody production against off-target MVs, we compared the levels of CPS14-specific immune responses between the groups of the intranasal MVs (vector control, Grp. A) and the intranasal CPS14+MVs (Grp. B). The serum and nasal wash samples at euthanasia were subjected to ELISA using plates coated with MVs (Fig. 4D). The results showed that the levels of CPS14-specific serum IgG and nasal wash IgA in the group of intranasal MVs (Grp. A) significantly increased compared to those in the PBS group (Grp. F). The CPS14-specific serum IgG and nasal

wash IgA were also observed in the intranasal CPS14+MVs (Grp. B), although no statistically significant difference was detected when compared to the PBS group (Grp. F). Notably, the levels of both serum IgG and nasal wash IgA in the intranasal CPS14+MV group (Grp. B) were obviously lower than those of the intranasal MV group (Grp. A). The findings demonstrate that the antigenicity of MVs significantly decreased by displaying CPS14 on MVs, suggesting the advantage of densely displayed polysaccharide antigens on the MV surface in the context of suppressing antibody induction against off-target MVs.

Groups	Vaccines	Routes	CPS14/dose	Numbers
■ Grp. A	MVs (vector control)	i.n.	None	n = 8
■ Grp. B	CPS14 <sup>+</sup> MVs	i.n.	0.013 µg	n = 8
■ Grp. C	CPS14 <sup>+</sup> MVs	s.c.	0.013 µg	n = 8
■ Grp. D	PCV	s.c.	0.039 µg	n = 8
■ Grp. E	PPSV	s.c.	4.5 µg	n = 8
□ Grp. F	PBS (mock immunization)	s.c.	None	n = 3

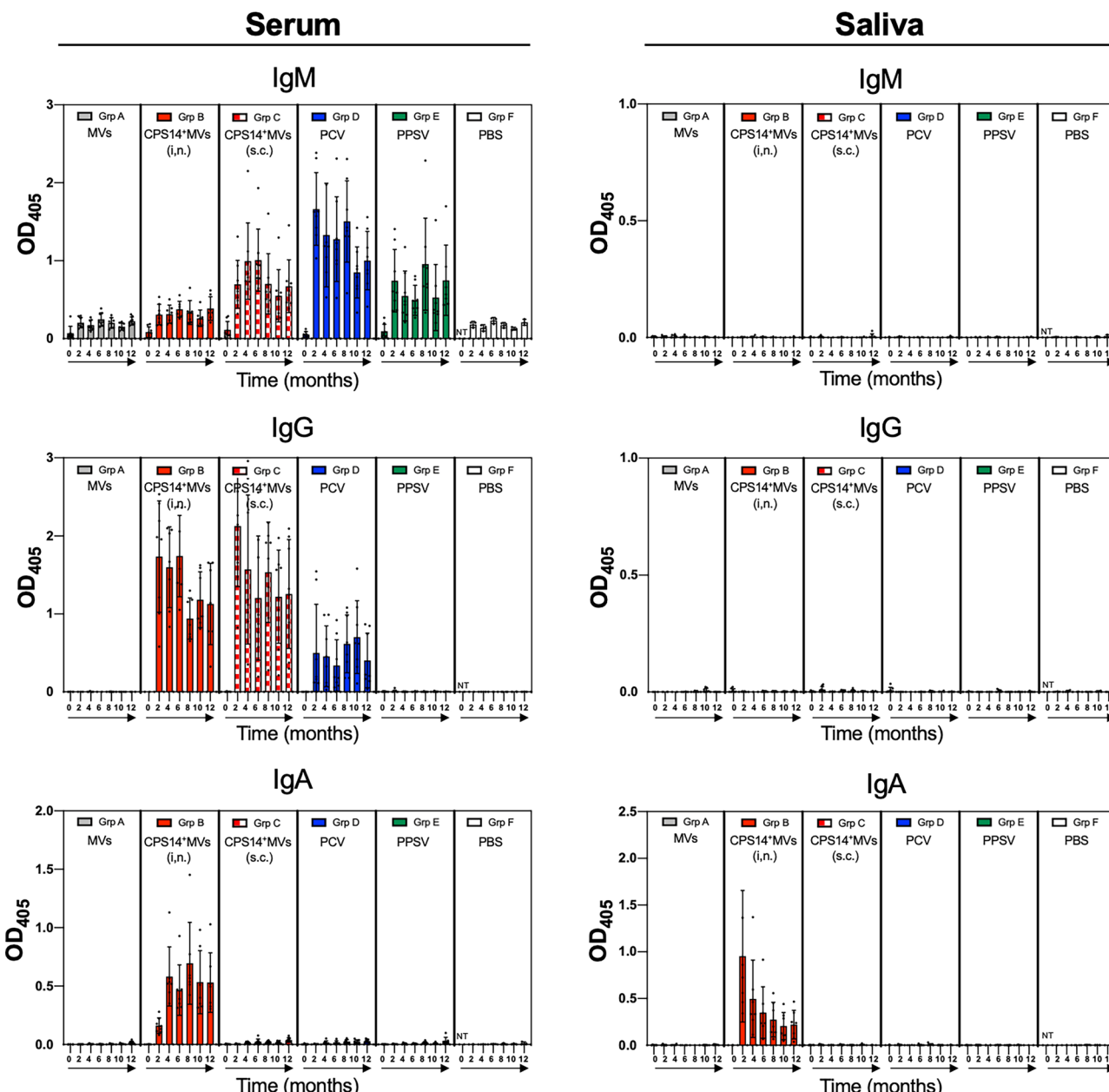


**Fig. 3 | One-year follow-up of antibody production in serum and saliva.** Shown are the results of ELISA using samples from 43 mice in the long-term animal experiments. See the timeline in Fig. 2B. Vaccination groupings of mice are described in the box table in the upper left, which shows the vaccine used, the route, the amount of CPS14 per dose, and the number of mice in each group. ELISA was performed using serum and salivary samples obtained from mice every 2 months. The y-axis of each panel shows CPS14-specific IgM, IgG, and IgA of serum and saliva samples, as OD<sub>405</sub> values. In all ELISAs

except for serum IgG, samples were used at 1:100 dilution. In the ELISA for serum IgG, the samples were used at 1:1000 dilution. The results of serum IgA, salivary IgM, IgG, and IgA ELISAs are expressed as OD<sub>405</sub> values (mean  $\pm$  SD) after a 120-min incubation with AP substrate. The results of serum IgM and IgG ELISAs are expressed as OD<sub>405</sub> values (mean  $\pm$  SD) after a 30-min incubation with AP substrate. The OD<sub>405</sub> values of individual mice are shown as small dots. One mouse in Grp. B died accidentally at week 8. Two mice in the Grp. E died accidentally at weeks 45 and 56. NT: Not tested.

#### Influence of aging on immune responses after intranasally or subcutaneously immunizing with CPS14<sup>+</sup>MVs

To compare the influence of aging on immune responses between the intranasal and the injected CPS14<sup>+</sup>MV vaccines, systemic and mucosal immunogenicity of CPS14<sup>+</sup>MV vaccine in old mice (54 weeks old) were

compared with those in young mice (7 weeks old) (Fig. 5). In subcutaneous immunization with CPS14<sup>+</sup>MV vaccine, all tested antibodies in serum, saliva, nasal wash and BALF were comparable between young and old mice. As in Figs. 3 and 4, subcutaneous immunization failed to induce CSR to IgA and produce IgA in saliva, nasal wash, and BALF in both young and old

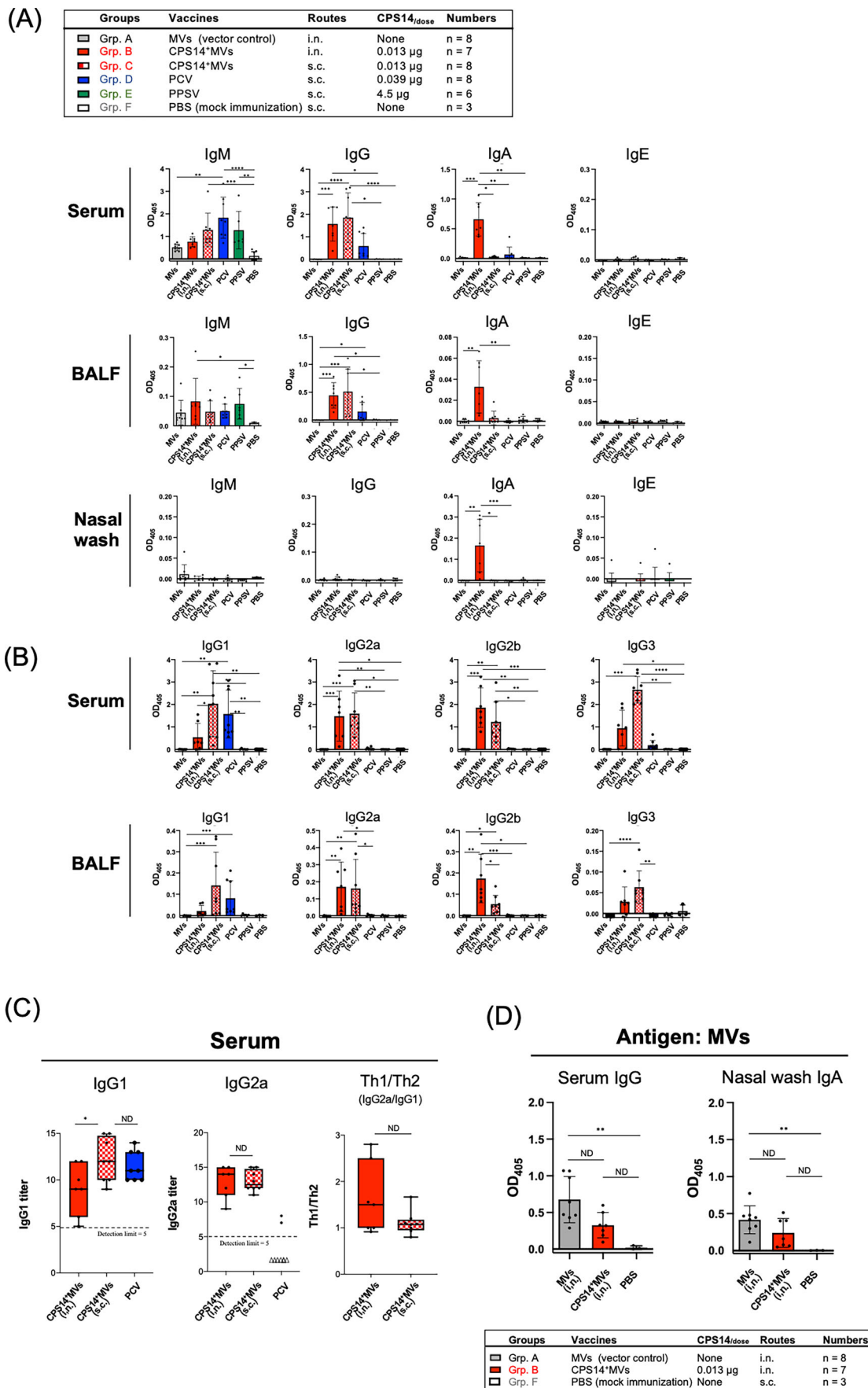


**Fig. 4 | Humoral immune responses in mice euthanized at the end of the long-term animal experiment.** A CPS14-specific IgM, IgG, IgA, and IgE antibodies in serum, BALF, and nasal wash samples in aged mice. As shown in the timeline of the long-term study (Fig. 2), the samples of serum, nasal wash, and BALF were collected from all mice at the end of the long-term animal experiment (after the bacterial clearance assay). The CPS14-specific antibodies in these samples were examined.

Vaccination groupings of mice are described in the box table in the upper left, which shows the vaccine used, the route, the amount of CPS14 per dose, and the number of mice in each group. The number of mice analyzed was eight in all groups except Grp. B ( $n = 7$ ) and Grp. E ( $n = 6$ ), due to the accidental deaths of one and two mice in Grps. B and E, respectively. In all ELISAs except for serum IgG, samples were used at 1:100 dilution. In the ELISA for serum IgG, the samples were used at 1:1000 dilution. The results of IgM and IgG ELISAs are expressed as OD<sub>405</sub> values (mean  $\pm$  SD) after a 30-min incubation with AP substrate. The results of IgA and IgE ELISAs are expressed as OD<sub>405</sub> values (mean  $\pm$  SD) after a 120-min incubation with AP substrate. Shown are the results of statistical analysis using Kruskal-Wallis test. \* $p < 0.05$ . \*\* $p < 0.01$ .

\*\*\* $p < 0.001$ . \*\*\*\* $p < 0.0001$ . Shown are the results from a series of samples of all the mice ( $n = 40$ ) obtained from one independent animal experiment. B CPS14-specific IgG subclass responses in serum and BALF. The serum and BALF samples from the mice ( $n = 40$ ) at euthanasia were also used for CPS14 ELISA to detect all IgG subclasses. Vaccination groupings of mice are described in the box table in the upper left, which shows the vaccine used, the route, the amount of CPS14 per dose, and the number of mice in each group. In all IgG subclass ELISAs, samples were used at a 1:100 dilution. The results are expressed as OD<sub>405</sub> values (mean  $\pm$  SD) after a 30-min incubation with AP substrate. Shown are the results of statistical analysis using the Kruskal-Wallis test.

\* $p < 0.05$ . \*\* $p < 0.01$ . \*\*\* $p < 0.001$ . \*\*\*\* $p < 0.0001$ . C Th1/Th2 profiles of CPS14-specific humoral immune responses. Titers of serum IgG1 and IgG2a, and Th1/Th2 ratio were compared between Grps B (MVs, i.n.,  $n = 7$ ), C (CPS14<sup>+</sup>MVs, s.c.,  $n = 8$ ), and D (PCV, s.c.,  $n = 8$ ). In the panel of “IgG1” or “IgG2a”, small dots represent the IgG1 or IgG2a endpoint titer, respectively. The endpoint titers are expressed as the reciprocal log<sub>2</sub> of the last dilution that provided an OD<sub>405</sub> of 0.05 greater than the background level, which was determined as the average of 2 control serum samples randomly chosen from the Grp. F mice (PBS, s.c.) in the same ELISA plate. The numbers of open triangles indicate the samples under the limit of detection, which was 5 (as log<sub>2</sub>). In the panel of “Th1/Th2”, small dots represent the values of IgG2a titer/IgG1 titer. For “IgG1” and “IgG2a”, shown are the results of the statistical analysis using Kruskal-Wallis test. For “Th1/Th2”, shown are the results of the statistical analysis using the Mann-Whitney *U*-test. In the box-and-whiskers plots, the box and the horizontal line in the boxes indicate the values of SD and median, respectively. The whiskers indicate the minimum and maximum values \* $p < 0.05$ . ND: no statistically significant difference. D MV-specific humoral immune responses. The serum and nasal samples from the mice of Grps. A (MVs, i.n.,  $n = 8$ ), B (CPS14<sup>+</sup>MVs, i.n.,  $n = 7$ ), and F (PBS, s.c.,  $n = 3$ ) were also examined to detect MV-specific antibodies. Vaccination groupings of mice are shown in the box table at the bottom, which shows the used vaccine, the route, the amount of CPS14 per dose, and the number of mice in each group. The serum and nasal wash samples were used at 1:1000 or 1:100 dilution, respectively. The results are expressed as OD<sub>405</sub> values (mean  $\pm$  SD) after a 30-min or 120-min incubation with AP substrate for serum IgG or nasal wash IgA, respectively. Shown are the results of statistical analysis using the Kruskal-Wallis test. \*\* $p < 0.01$ . ND: no statistically significant difference.

mice. In intranasal immunization with CPS14<sup>+</sup>MV vaccine, an age-related decline in serum IgG level was observed. There was also a tendency for weaker CSR to IgA in old mice as compared with young mice. Overall, potent CPS14-specific immune responses were observed even when old mice were intranasally immunized with CPS14<sup>+</sup>MVs, suggesting that the intranasal CPS14<sup>+</sup>MV vaccine may be effective even in aged mice with immune senescence.

#### Opsonophagocytic activity of serum antibodies in vaccinated mice

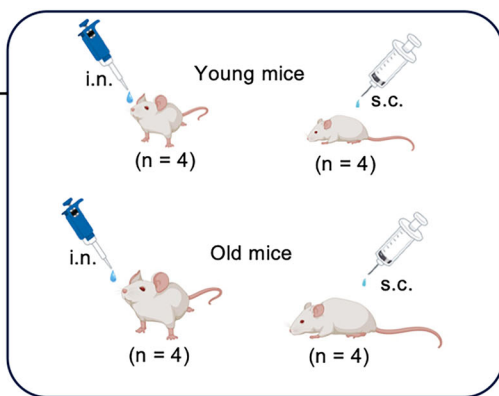
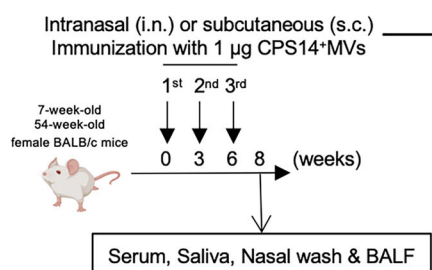
To assess the killing activity of serum of mice immunized with different vaccines, we examined the opsonophagocytic activity against a serotype 14 pneumococcal strain (Fig. 6). The serum samples used were obtained from all mice in the seven groups of the long-term animal experiments at euthanasia after infection experiment (see the timeline in Fig. 2). The activity was detected in all vaccinated groups. A significantly higher opsonic index (OI) value was detected in the injected CPS14<sup>+</sup>MV group (Grp. C) compared to the PPSV23 subcutaneous vaccine group (Grp. E) (Fig. 6A), while no significant differences were observed among the other vaccinated groups (Fig. 6A). Moreover, the correlation between opsonophagocytic activity and various antibody classes/subclasses was assessed by linear regression analysis, and r-squared values were calculated (Fig. 6B). The strongest positive correlation was observed between OI value and IgG ( $R^2 = 0.6914$ ,  $P < 0.0001$ ). Strong positive correlations were also observed between OI value and IgG1 ( $R^2 = 0.5046$ ,  $P < 0.0001$ ), IgG2a ( $R^2 = 0.3421$ ,  $P < 0.001$ ), and IgG3 ( $R^2 = 0.2650$ ,  $P < 0.01$ ), whereas a relatively weak correlation was observed between OI value and IgG2b ( $R^2 = 0.1039$ ,  $P < 0.0881$ ), although no significant difference was observed. No correlation was detected between OI value and IgM ( $R^2 = 0.0399$ ,  $P < 0.2911$ ) or IgA ( $R^2 = 0.0005$ ,  $P < 0.9056$ ). However, irrespective of no detectable IgG responses in the PPSV23 group (Grp. E), those serum samples showed the opsonophagocytic activity. So, the correlation between opsonophagocytic activity and IgM was assessed in the Grp. E. We observed a very strong positive correlation between OI value and IgM ( $R^2 = 0.9514$ ,  $p < 0.0001$ ), suggesting that opsonophagocytic activity found in the PPSV23 mice (Fig. 6) is dependent on IgM.

#### Bacterial clearance in the nasal cavity of mice intranasally immunized with CPS14<sup>+</sup>MV vaccine

To determine whether the intranasal CPS14<sup>+</sup>MV vaccine can prevent pneumococcal colonization in the upper respiratory tract, we first

compared bacterial clearance at different time points after infection with a serotype 14 pneumococcal strain ATCC 700676 (Fig. S3A). As controls, mice were intranasally immunized with MVs (vector control) and were also subcutaneously immunized with PCV13 (Fig. S3A). Intranasal CPS14<sup>+</sup>MVs elicited stronger CPS14-specific IgG and IgA responses than intranasal MVs and the subcutaneous PCV13. The high levels of serum IgG and IgA in the intranasal CPS14<sup>+</sup>MV group were maintained until day 7 after infection (Fig. S3B). The CFU results at day 1 showed less variation than those at days 3 and 7 (Fig. S3). In addition, a significant difference between the groups of intranasal CPS14 MVs and subcutaneous PCV13 was observed at day 1 (Fig. S3). From the findings, the timepoint at day 1 was chosen. Based on the results of Fig. S3, the upper respiratory tract infection experiments were set up at the end of the long-term experiment (Figs. 2B and 7A). The number of pneumococci in the nasal wash obtained 24 h after challenge was calculated using both CFU counting and real-time PCR assays (Fig. 7B). A positive correlation was observed between the two assays using nasal wash samples (Fig. S4,  $R^2 = 0.7770$ ,  $P < 0.0001$ ). Bacterial clearance in the nasal cavity was successful in the intranasal CPS14<sup>+</sup>MV vaccine (Grp. B), whereas all the other groups failed to clear pneumococci from the nasal cavity. The intensity of clearance did not correlate with the antibody levels in serum, saliva, nasal wash, or BALF samples for any of the antibody classes or IgG subclasses (Fig. S5). Nevertheless, SIgA production in the upper respiratory tract may be involved in respiratory defense. We therefore performed the same upper respiratory tract infection experiments in wild-type (*pIgR*<sup>+/+</sup>) and the *pIgR*-knockout (*pIgR*<sup>-/-</sup>) mice (Fig. 8A), which cannot release SIgA into the nasal cavity, because *pIgR* facilitates the translocation of IgA from the lamina propria to the mucosal surface. By serum immunoglobulin profiling, lack of SIgA secretion into the nasal cavity was confirmed in *pIgR*<sup>-/-</sup> mice; instead, elevated serum IgA was detected in *pIgR*<sup>-/-</sup> mice compared to *pIgR*<sup>+/+</sup> mice (Fig. S6). On the other hand, the serum IgG level of *pIgR*<sup>-/-</sup> mice was comparable to that of *pIgR*<sup>+/+</sup> mice (Fig. S6). In the challenge experiments, *pIgR*<sup>+/+</sup> mice intranasally immunized with CPS14<sup>+</sup>MV vaccine were protected from pneumococcal colonization of the nasal cavity (Fig. 8B). However, the same vaccine regimen failed to protect *pIgR*<sup>-/-</sup> mice from pneumococcal colonization (Fig. 8B). In the CFU counting assay using BALF, no colony was not detected from BALF samples of all mice used in the present study, showing that no leakage of pneumococci into the lung was confirmed in our *in vivo* respiratory tract infection model (data not shown).

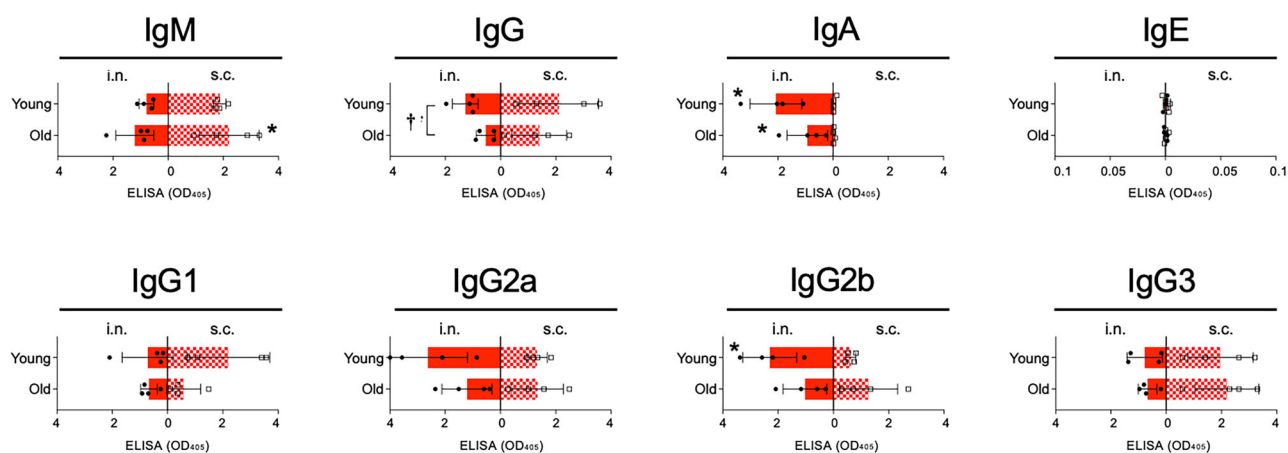
(A)



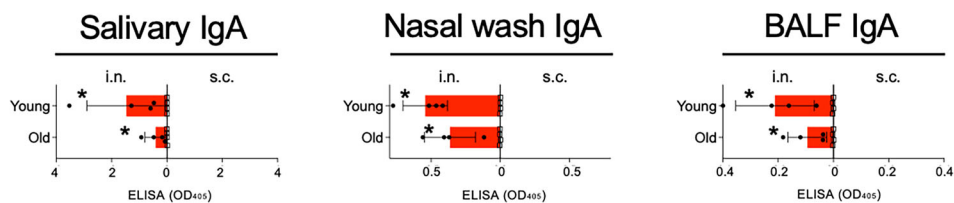
\*The ELISA results in young and old mice subcutaneously immunized with CPS14<sup>+</sup>MVs have been previously published (Nakao R et al. 2022). These samples were re-analyzed in comparison to those of intranasally immunized with CPS14<sup>+</sup>MVs in the present study. The experiments of young and old mice intranasally immunized with CPS14<sup>+</sup>MVs were performed at a same moment as the previously published experiments of young and old mice subcutaneously immunized with CPS14<sup>+</sup>MVs.

(B)

### Serum



(C)



### Discussion

Pneumococcal colonization of the nasopharynx is a prerequisite not only for common respiratory tract infections, such as otitis, sinusitis, and community-acquired pneumonia, but also for IPD; i.e., life-threatening septicemia and meningitis. The injected vaccines currently available are excellent in that they efficiently induce IgM and IgG; however, they are not primarily intended to induce SIgA, which may prevent pneumococcal colonization of the nasopharynx. In contrast, intranasal vaccines can activate immune cells in the mucosal tissues of the nasopharynx and recruit tissue-resident memory B cells that produce SIgA in the upper respiratory tract. However, it is unclear how well SIgA protects against pneumococci. In the present study, only the intranasal CPS14<sup>+</sup>MV vaccine achieved pneumococcal clearance in the nasal cavity of mice, whereas the other injected

vaccine regimens failed to protect against pneumococcal colonization (Fig. 7). On the other hand, the upper respiratory tract was colonized by pneumococci when *plgR*<sup>-/-</sup> mice that lack SIgA production were used (Fig. 8). These findings suggested that SIgA-dependent clearance is essential for achieving sterilizing immunity against pneumococci in mice.

Decreased immunity in elderly individuals is an important medical concern for the aging population. Despite several advances in the field of pneumococcal vaccinology, the current CPS-based vaccines are often poorly immunogenic and not durable in the elderly<sup>25,26</sup>. In an *in vivo* experiment, old mice did not effectively clear pneumococcal colonization in the nasopharynx in a previous report<sup>27</sup>. The present MV-based polysaccharide vaccine strongly elicited antibody production, irrespective of the age difference, both in the bloodstream and at mucosal surfaces (oral cavity, upper

**Fig. 5 | Humoral immune responses of young and old mice.** A Timeline of vaccine regimen to young (7 weeks old) and old (54 weeks old) mice. Female BALB/c mice aged at 7 weeks old ( $n = 8$ ) and 54 weeks old ( $n = 8$ ) were used in this study. The young mice ( $n = 8$ ) and old mice ( $n = 8$ ) were equally distributed into two groups, and were intranasally (i.n.,  $n = 4$ ) or subcutaneously (s.c.,  $n = 4$ ) immunized with 1  $\mu$ g of CPS14<sup>+</sup>MVs, respectively. One  $\mu$ g of CPS14<sup>+</sup>MVs contained 0.013  $\mu$ g of CPS14. Vaccination was performed three times at 3-week intervals (weeks 0, 3, and 6). Serum and saliva samples were collected at week 8. The results of ELISA in young and old mice subcutaneously immunized with CPS14<sup>+</sup>MVs have been previously published<sup>24</sup>. These samples were re-analyzed in comparison to those of intranasally immunized with CPS14<sup>+</sup>MVs in the present study. The experiments of young and old mice intranasally immunized with CPS14<sup>+</sup>MVs were performed at the same time as the previously published experiments of young and old mice subcutaneously immunized with CPS14<sup>+</sup>MVs. Representative data shown in **B** and **C** were obtained from the young mice ( $n = 8$ ) and old mice ( $n = 8$ ) in one independent animal experiment. Created in BioRender. Konig, S. (2025) <https://BioRender.com/z8u1cwz>. **B** CPS14-specific antibodies in serum samples. In all

ELISAs except for IgG, serum samples were used at a 1:100 dilution. In the ELISA for serum IgG, the samples were used at a 1:1000 dilution. The results are expressed as OD<sub>405</sub> values (mean  $\pm$  SD). Incubation time after AP substrate addition was as follows: Serum IgM (90 min), Serum IgG (45 min), Serum IgA (120 min), Serum IgE (120 min), Serum IgG1 (90 min), Serum IgG2a (90 min), and Serum IgG2b (45 min), Serum IgG3 (60 min). Asterisks denote a statistically significant difference ( $p < 0.05$ ) between intranasal and subcutaneous administrations. A dagger in the panel of serum IgG denotes a statistically significant difference ( $p < 0.05$ ) between young and old mice when intranasally vaccinated with CPS14<sup>+</sup>MVs. Shown are the results of the statistical analysis using the Mann-Whitney *U*-test. **C** CPS14-specific IgA in saliva, nasal wash, and BALF samples. Saliva, nasal wash, and BALF samples were used at a 1:100 dilution. The results are expressed as OD<sub>405</sub> values (mean  $\pm$  SD). Incubation time after AP substrate addition was as follows: Salivary IgA (120 min), Nasal wash IgA (120 min), and BALF IgA (120 min). Asterisks denote statistically significant difference ( $p < 0.05$ ) between intranasal and subcutaneous administrations. Shown are the results of statistical analysis using the Mann-Whitney *U*-test.

and lower respiratory tracts), which are the primary sites for pneumococcal colonization, when the vaccine is administered intranasally (Fig. 5). In addition, not only do all IgG subclasses persist in blood, but also IgA also in the oral cavity, nasal cavity, and lung have been persisted through the one-year timeframe (Figs. 3 and 4). Therefore, the intranasal MV-based vaccine regimen may provide optimal protection against pneumococcal disease for subjects with declined immunity, such as the elderly and immunocompromised patients.

Intranasal immunization with purified CPS14 (Fig. 1), as well as PCVs (data not shown), induced only a weak IgM response, but neither IgG nor IgA was produced. On the other hand, our glycoengineered MV-based approach could induce stronger IgG/IgA responses (Fig. 1), resulting in positive results in both opsonophagocytic killing (Fig. 6) and bacterial clearance assays (Fig. 7). These advantages may be attributed to at least three characteristics of the MVs: particle size of MVs, surface-arrayed epitopes on MVs, and pathogen-associated molecular patterns (PAMPs) in MVs. First, the MV size, ranging from 40 to 80 nm in diameter (average: 63.5 nm)<sup>24</sup> closely resembles that of a typical virus, which might contribute to the efficient uptake of intranasally administrated antigens from antigen-presenting cells, as well as the efficient travel from the interstitial tissue into lymphatic vessels, followed by accumulation within local lymph nodes<sup>28–30</sup>. In addition, Munoz-Wolf et al. recently reported that the optimal size of poly(lactic-co-glycolic acid) (PLGA)-based particles for induction of Th1-type responses was 50–60 nm in diameter<sup>31</sup>, which is in good agreement with the MV size used in this study. Second, the glycoengineered pneumococcal CPS14 moiety on the MVs is highly organized and polymerized like the O-antigen of LPS, and covalently tethered on the outermost surface at high density<sup>24</sup>, which might allow for efficient B cell receptor (BCR) cross-linking<sup>32,33</sup> with highly repetitive epitopes on the MVs, followed by protective IgG and IgA responses (Figs. 6 and 7). Third, PAMPs of MVs are considered to provide intrinsic adjuvanticity. The EcN MVs showed an immunostimulatory effect on host immune cells via TLR2/4 and NOD1<sup>34,35</sup>. However, further studies are required for elucidation of the activation mechanism by the intranasal MV-based vaccines.

In the present study, the optimal intranasal dose of CPS14<sup>+</sup>MVs for BALB/c mice was determined to be 1  $\mu$ g (Fig. S1). The amount of CPS14 in 1  $\mu$ g of CPS14<sup>+</sup>MVs was 0.0013  $\mu$ g, which was equivalent to 1/30 and 1/350 of CPS14 contained in undiluted PCV and PPSV solution, respectively, which contains 0.39  $\mu$ g CPS14/dose and 4.5  $\mu$ g CPS14/dose, respectively. In light of the need to reduce polysaccharide dosage and the prospect of developing higher-valency vaccines, the present MV vaccine modality could offer significant advantages over the two conventional PCV and PPSV vaccines.

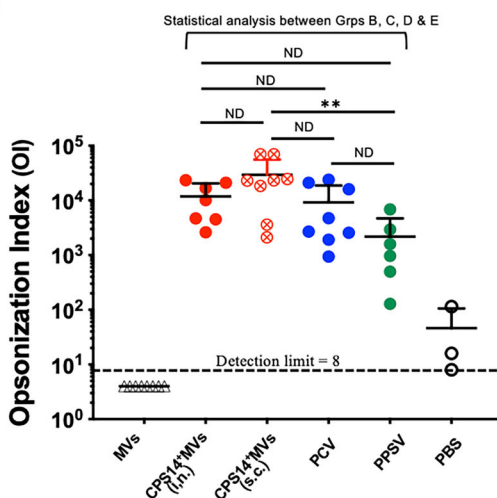
In Fig. 4, in vivo infection by pneumococci might lead not only to immune responses, but also to antibody consumption in the nasal cavity by binding the bacterial surface. To rule out the possibility that infection substantially affects the amount of antibodies, we compared the ELISA

results before and after infection. The trends of the IgM, IgG, and IgA responses in serum and BALF samples of each group one day after infection (Fig. 4A, at 14 or 15 months after the 1st immunization) were similar to those in serum IgM, IgG, and IgA using the samples collected at the last time point before infection (Fig. 3, at 12 months). In addition, the trend of IgA responses in nasal wash samples (Fig. 4A, at 14 or 15 months) was similar to those in IgA in saliva (Fig. 3, at 12 months) and eye wash (Fig. S2, at 13 months). Furthermore, no significant difference in humoral immune responses of sera was observed between 1, 3, and 7 days after challenge in an independent animal experiment (Fig. S3). Therefore, the influence of the bacterial load used in this study ( $2 \times 10^5$  CFU/mouse) on antibody production as well as antibody consumption was considered negligible.

The introduction of vaccine programs against various respiratory tract infections has reduced the disease burden globally<sup>7</sup>. Pneumococcal vaccines are also an example of successful vaccines that contributed significantly to reducing mortality and morbidity<sup>17</sup>. However, global inequities in vaccine access were amplified not only for the COVID-19 vaccine during the pandemic<sup>36,37</sup>, but also for pneumococcal vaccines<sup>7</sup>, mainly due to the high cost of pneumococcal vaccine manufacturing and distribution to the people in low- and middle-income countries (LMICs) that were not supported by GAVI<sup>38</sup>. Considering the challenge of vaccine dissemination worldwide, an intranasal MV-based vaccine would be a suitable platform, because only low-cost syringes without needles are required for nasal administration, and the vaccine can be administered by patients. The thermostability of MVs<sup>24</sup> is another advantage, in stark contrast to the heat-labile nature of mRNA vaccines. *E. coli* can efficiently produce endotoxin-depleted MVs by the glycine induction method<sup>22,23</sup>, which yields several dozen milligrams of MVs from one liter of culture<sup>24</sup>, corresponding to more than 10,000 and 1000 doses for immunization of mice and humans, respectively (if the extrapolation factor from mice to humans is set to 10). Taken together, the cost-effectiveness and thermo-stability of the MV-based vaccine platform could contribute to vaccine dissemination to more countries.

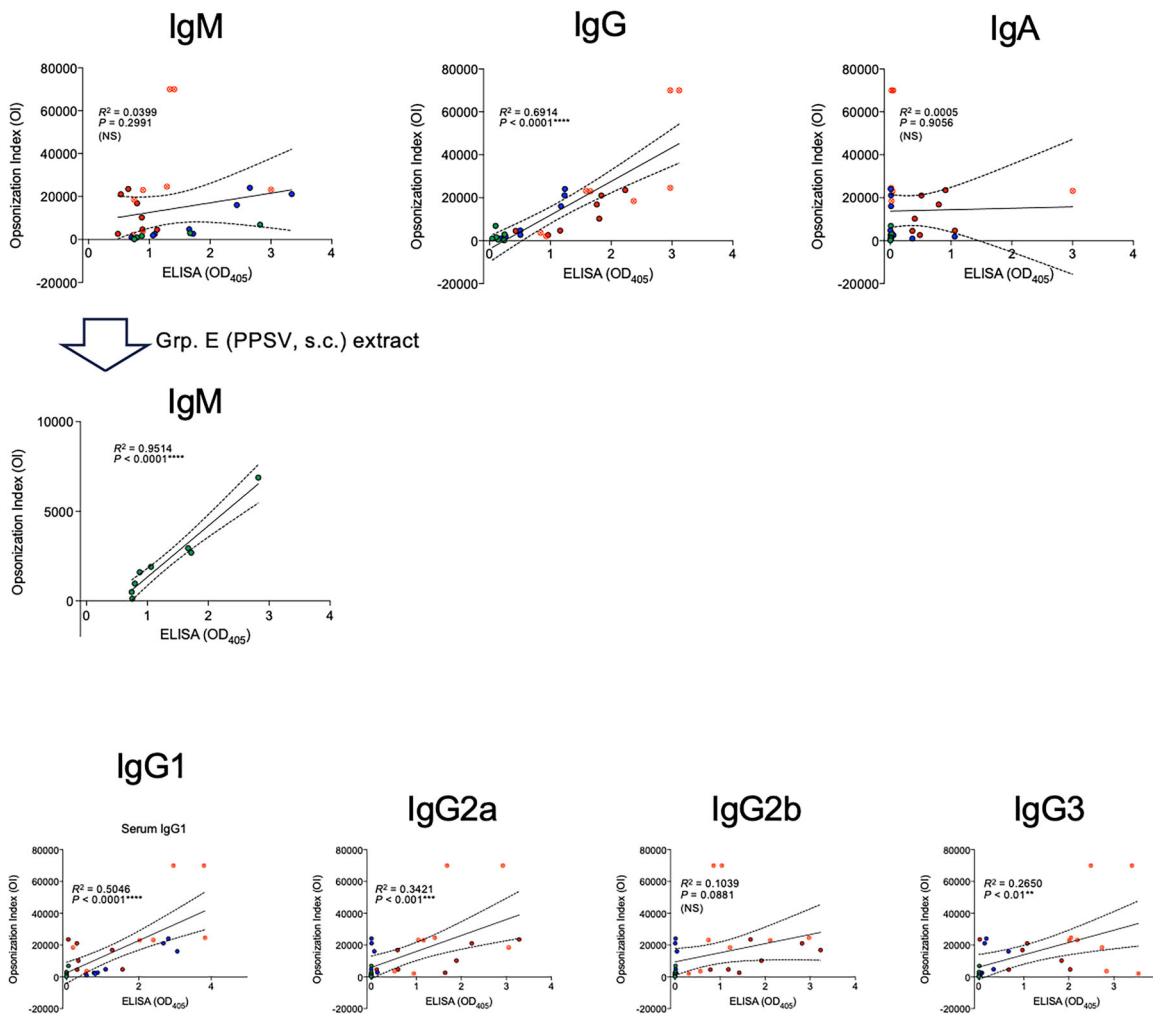
In wild-type (*pIgR*<sup>+/+</sup>) mice intranasally immunized with MVs (vector control), pneumococci colonized the nasal cavity of most animals as assessed by real-time PCR (Fig. 8). In contrast, in the *pIgR*<sup>-/-</sup> mice, pneumococci failed to colonize in the nasal cavity in half the animals in both the CFU counting and real-time PCR assays (Fig. 8). One possible reason for this is that *pIgR* functions as the receptor of epithelial/endothelial cells for two molecules of pneumococci essential for colonization: choline-binding protein A (CbpA) and pilus-1 adhesin protein (RrgA). Zhang et al. reported that pneumococcus binds to human *pIgR* and promotes translocation into epithelial cell lines<sup>39</sup>. CbpA, also known as PspC<sup>40</sup> or SpsA<sup>41</sup>, binds to human *pIgR* and adheres to epithelial cell lines, with binding mediated by the YRNYP motif of CbpA. However, CbpA does not bind to mouse *pIgR*<sup>42</sup>. On the other hand, RrgA is involved in the adhesion of *Streptococcus pneumoniae* to the host cells<sup>43</sup>. *pIgR* expressed on the surface of human cells and platelet endothelial cell adhesion molecule (PECAM-1) are the two host

(A)



Groups	Vaccines	CPS14/dose	Routes	Numbers
• Grp. A	MVs (vector control)	None	i.n.	n = 8
• Grp. B	CPS14* MVs	0.013 µg	i.n.	n = 7
• Grp. C	CPS14* MVs	0.013 µg	s.c.	n = 8
• Grp. D	PCV	0.039 µg	s.c.	n = 8
• Grp. E	PPSV	4.5 µg	s.c.	n = 6
○ Grp. F	PBS (mock immunization)	None	s.c.	n = 3

(B)



receptors that bind to RrgA<sup>44</sup>. So, at least for RrgA, it may function as a receptor for both human and mouse pIgR. Given the reports demonstrating the importance of pIgR-mediated pneumococcal adhesion, *pIgR*<sup>-/-</sup> mice, which lack pIgR expression in the upper respiratory tract, were thought to be less susceptible to pneumococcal colonization compared to wild-type mice.

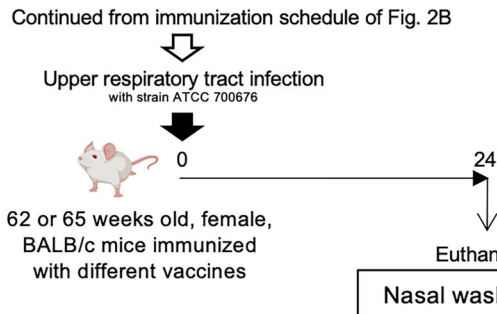
The present study has several limitations. First, whereas the current PCVs and PPSVs contain multiple antigens of different CPS serotypes, only one serotype of CPS (CPS14) was investigated in this study. The present EcN mutant strain produced MVs displaying plenty of the exogenous CPS14 that were covalently tethered to a lipid A-core oligosaccharide anchor of LPS<sup>24</sup>, however, it has not been tested whether

**Fig. 6 | Opsonophagocytosis of serum samples of vaccinated mice.**

A Opsonophagocytic activity in serum samples of mice at the end of the long-term experiment. Serum samples collected from the 40 mice after the bacterial clearance assay were used for the opsonophagocytic killing assay. Vaccination groupings of mice are described in the right table, which shows the vaccine used, the amount of CPS14 per dose, the route, and the number of mice in each group. The y-axis shows the opsonization index (OI) of each data (circle) and the average with SD (horizontal bar) in the group. OI was defined as the reciprocal of the serum dilution that killed 50% of the test bacteria. Open triangles indicate the samples under the detection

limit of the OI, which was 8. Shown are the results of the average statistical analysis between all groups except Grps. A and F, using the Kruskal-Wallis test.  $^{**}p < 0.01$ . ND: no statistically significant difference. B Correlations of the OI with the  $OD_{405}$  values in CPS14 ELISA. Representative data were generated from the results of ELISA (Fig. 4) and OPA (A) using only 29 serum samples from vaccinated groups (Grps. B–E) after bacterial clearance assay. Focusing on the PPSV23 group (Grp. E), the association between the IgM responses and opsonophagocytic activity was also analyzed. Shown are the plotted values with the linear regression line with the  $R^2$  and  $p$  values.

(A)



Groups	Vaccines	CPS14/dose	Routes	Numbers
• Grp. A	MVs (vector control)	None	i.n.	n = 8
• Grp. B	CPS14+MVs	0.013 µg	i.n.	n = 7
• Grp. C	CPS14+MVs	0.013 µg	s.c.	n = 8
• Grp. D	PCV	0.039 µg	s.c.	n = 8
• Grp. E	PPSV	4.5 µg	s.c.	n = 6
• Grp. F	PBS (mock immunization)	None	s.c.	n = 3

(B)

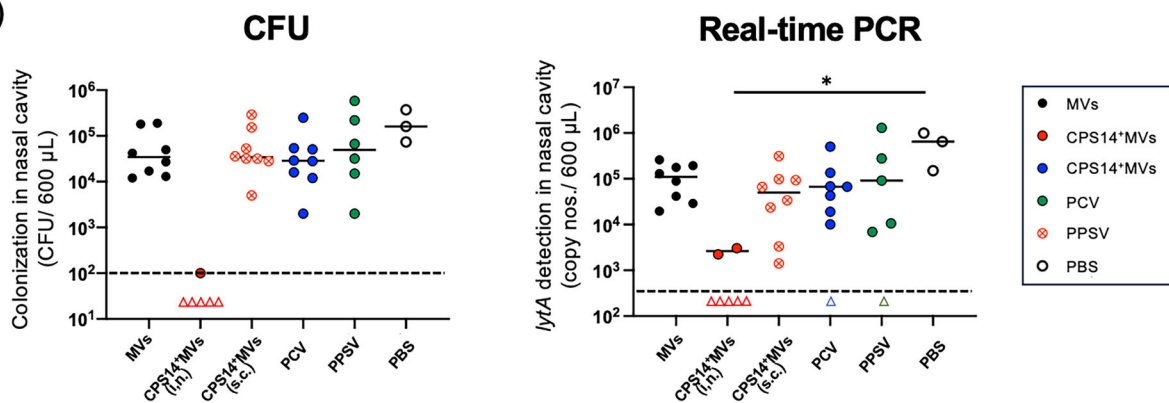
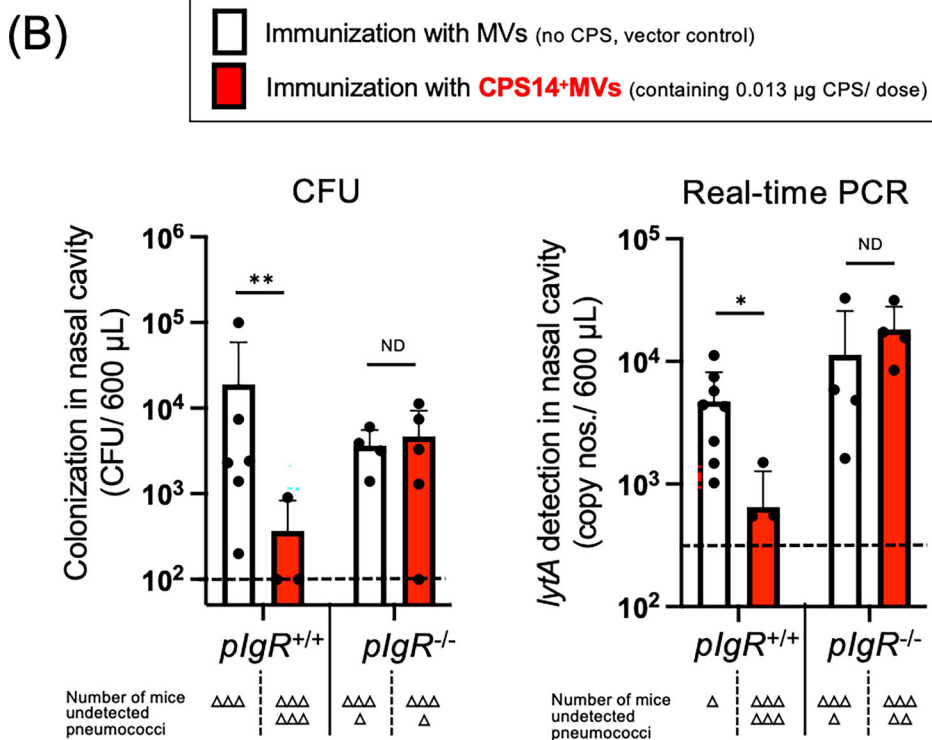
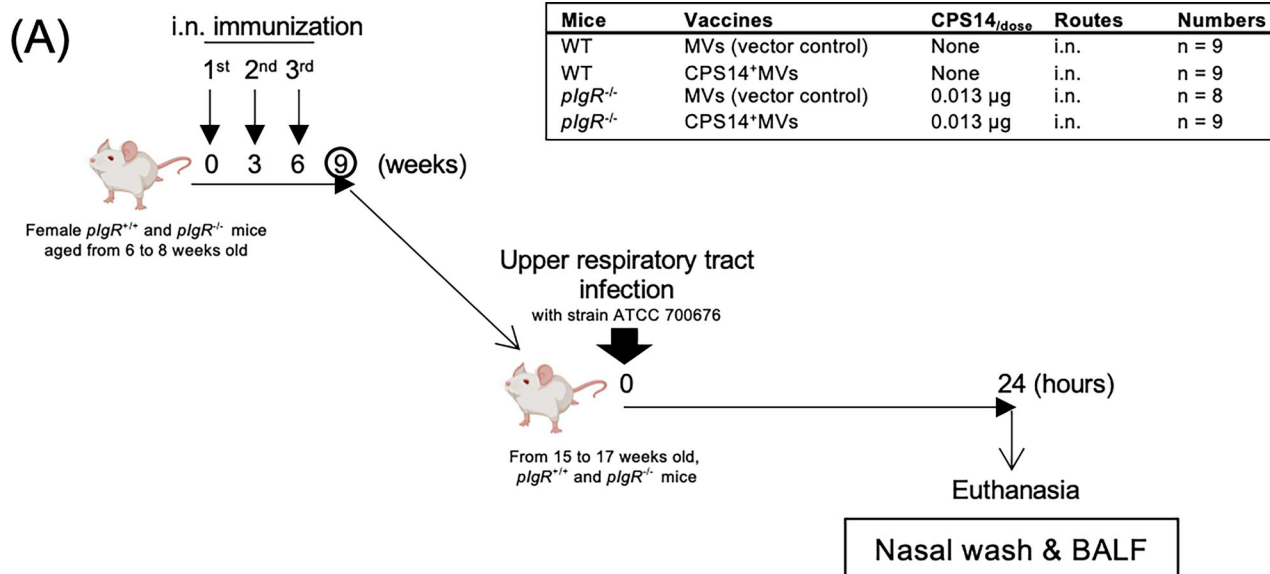


**Fig. 7 | Protection from pneumococcal infection in aged mice.** Timeline of challenges with pneumococci and sample collection. In the continuation of Fig. 2B, all the aged mice that survived ( $n = 40$ ) were intranasally inoculated with a serotype-14 pneumococcal strain ATCC 700676 at a dose of  $2 \times 10^5$  CFU. Vaccination groupings of mice are described in the right table, which shows the vaccine used, the amount of CPS14 per dose, the route, and the number of mice in each group. Twenty-four hours after the inoculation, the mice were euthanized, and the amount of pneumococci in the nasal wash and BALF samples was analyzed. Due to there being too many mice to perform the experiment at once, the 40 mice were divided into two groups: Class I and Class II. The bacterial clearance assay using mice of Class I and Class II was performed at 62 and 65 weeks old, respectively. The number of mice allocated to Class I was 18: Grp. A ( $n = 3$ ), Grp. B ( $n = 3$ ), Grp. C ( $n = 3$ ), Grp. D ( $n = 3$ ), Grp. E ( $n = 3$ ), and Grp. F ( $n = 3$ ). The number of mice allocated to Class II was 22: Grp. A ( $n = 5$ ), Grp. B ( $n = 4$ ), Grp. C ( $n = 5$ ), Grp. D ( $n = 5$ ), and Grp. E ( $n = 3$ ). Created in BioRender. Konig, S. (2025) <https://BioRender.com/z8u1cwz>. B Bacterial clearance in the nasal cavity

(Left) The number of live pneumococci (CFU/600 µL) in the nasal cavity was enumerated by CFU counting. The y-axis shows the CFU data of each sample (circle) and the average (horizontal bar) in the group. Open triangles indicate the samples under the limit of detection ( $10^2$  CFU). No pneumococcus was detected in 6 of 7 nasal wash samples in Grp. B. No pneumococcus was detected in any of the BALF samples in all the groups (right). The number of pneumococci (the copy number of the *lytA* gene/600 µL) in the nasal cavity was also determined by *lytA*-targeted real-time PCR. The y-axis shows the copy number of each sample (circle) and the average (horizontal bar) in the group. Open triangles indicate the samples under the limit of detection, which was 495 copies. No *lytA* gene was detected in nasal washes in 5 of 7 mice in Grp. B, 1 of 8 mice in Grp. D, and 1 of 6 mice in Grp. E. Shown are the combined results from the two independent animal experiments: Class I (week 62,  $n = 22$ ) and II (week 65,  $n = 28$ ). Shown are the results of the statistical analysis using the Kruskal-Wallis test.  $^{*}p < 0.05$ . No colony on the blood agar was detected from all the BALF samples (data not shown).

serotypes other than serotype 14 can also be densely expressed on MVs. Further investigation is required into the general applicability of the present MV glycoengineering, *i.e.*, the capability of the CPS translocation to the outer leaflet of the outer membrane. Second, the present study did not directly address the issue of serotype replacement, which is a major concern for future pneumococcal vaccine development. On the other hand, in the light of cross-reactivity of antibody, SIgA is more effective than monomeric IgA or IgG in neutralizing influenza viruses in

in vitro/in vivo animal models<sup>45,46</sup>, as well as in humans<sup>47</sup>. Higher order polymerization of mucosal SIgA, *e.g.*, tetramerization, improved the breadth of influenza viruses targeted<sup>48</sup>. Therefore, we consider that the resultant cross-reactive SIgA may provide broader infection prevention, which may also contribute to preventing immune escape caused by vaccination-induced selective pressure. Another limitation is that all the tested CPS-targeting vaccines are, of course, ineffective against nonencapsulated pneumococci, which are clinically relevant because



they comprise ~3–19% of asymptomatic carriage isolates and harbor multiple antibiotic resistance genes<sup>49</sup>. Moreover, in Fig. 4B, the MV-specific antibody was detected in mice intranasally vaccinated with MVs and CPS14<sup>+</sup>MVs. It is therefore necessary to carefully investigate whether MV vaccines generate off-target MV-specific antibodies in the context of safety in humans, prior to clinical trial launch. On the other hand, we found that MV-specific antibody production was significantly inhibited when CPS14 was densely displayed on MVs (Fig. 4D). The finding may pave the way to address potential adverse reactions caused by MV-specific antibody production.

## Methods

### Study design

The main objectives of the present study were to evaluate protective immunity elicited by intranasal MV vaccines produced from a chimeric probiotic *E. coli* expressing serotype-14 pneumococcal capsular polysaccharides. Pneumococcal CPS14-expressing MVs were isolated as spherical nanostructures by ultracentrifugation of culture supernatant of the probiotic *E. coli* strain derivative that harbors an expression vector containing a CPS14-biosynthesis gene cluster. BALB/c mice were intranasally immunized with chimeric CPS14<sup>+</sup>MVs, and the immunogenicity was

**Fig. 8 | Protection from pneumococcal infection fails in *pIgR*<sup>-/-</sup> mice even when vaccinated with CPS14<sup>+</sup>MVs.** A Timeline of immunization, challenge with pneumococci, and sample collection. Six- to 8-week-old female *pIgR*<sup>+/+</sup> and *pIgR*<sup>-/-</sup> mice were vaccinated with MVs (vector control) or CPS14<sup>+</sup>MVs three times at weeks 0, 3, and 6. At week 9, all the mice were intranasally inoculated with pneumococcal strain ATCC 700676 at the CFU of  $2 \times 10^5$ . Vaccination groupings of mice are described in the right table, which shows the vaccine used, the amount of CPS14 per dose, the route, and the number of mice in each group. Twenty-four hours after infection, mice were euthanized, and the nasal wash and BALF samples were collected. Created in BioRender. Konig, S. (2025) <https://BioRender.com/z8u1cwz>. B Bacterial clearance in the nasal cavity of *pIgR*<sup>+/+</sup> and *pIgR*<sup>-/-</sup> mice intranasally immunized with MVs (vector control) or CPS14<sup>+</sup>MVs. The nasal wash samples were analyzed by the CFU assay (left panel) and the real-time PCR assay (right panel). Representative data obtained from the *pIgR*<sup>+/+</sup> mice ( $n = 18$ ) and *pIgR*<sup>-/-</sup> mice ( $n = 17$ ) are the combined

results from 3 independent animal experiments. In total, 6- to 8-week-old female *pIgR*<sup>+/+</sup> mice ( $n = 18$ ) and *pIgR*<sup>-/-</sup> mice ( $n = 17$ ) were used in this study. The number of the *pIgR*<sup>+/+</sup> mice vaccinated with MVs (vector control) or CPS14<sup>+</sup>MVs was 9. The number of *pIgR*<sup>-/-</sup> mice vaccinated with MVs (vector control) or CPS14<sup>+</sup>MVs was 8 or 9, respectively. Shown are the individual data (dots) and mean with SD (bars) of the CFU/600  $\mu$ L (left panel) and the copy numbers of the *lytA* gene/600  $\mu$ L (right panel) in the nasal washes of *pIgR*<sup>+/+</sup> mice and *pIgR*<sup>-/-</sup> mice, which were immunized with MVs (white bars) or CPS14<sup>+</sup>MVs (red bars). The numbers of open triangles indicate the samples under the limit of detection, which was  $10^2$  CFU (left panel) and 495 copies (right panel) in the CFU and real-time PCR assays, respectively. Asterisks denote statistically significant differences. Shown are the results of statistical analysis using the Mann-Whitney *U*-test. \* $P < 0.05$ . \*\* $P < 0.01$ . ND: no statistically significant difference. No colony on the blood agar was detected from all the BALF samples (data not shown).

evaluated by ELISA using serum and saliva samples every 8 weeks for one year. As a control, mice were subcutaneously immunized with the two licensed pneumococcal vaccines: PPSV and the pneumococcal conjugate vaccine (PCV). Both contain the CPS14 antigen. In the latter part of the study, *pIgR* knock-out mice were also used. To highlight potential differences between the intranasal MV vaccine and other vaccines, vaccine effectiveness was assessed by opsonophagocytic activity, as well as by bacterial clearance in the nasal cavity.

#### Bacterial strains and growth conditions

A probiotic *E. coli* strain, Nissle 1917 (DSM 6601, serotype O6: K5:H1<sup>50</sup>), which does not produce flagella (EcN $\Delta$ flhD), was used to produce MVs. The EcN $\Delta$ flhD strain was transformed with a low-copy plasmid pWSK129<sup>51</sup> (vector control) or the derivative plasmid pNLP80, which contains an entire locus responsible for biogenesis of serotype-14 pneumococcal capsular polysaccharides (CPS14)<sup>52</sup>, which is included as one of the multi-serotypes in the current polyvalent pneumococcal vaccine formula as one of the most frequent serotypes that cause invasive pneumococcal diseases<sup>53</sup>. Both pWSK129 and pNLP80 carry a kanamycin-resistance marker and an isopropyl- $\beta$ -( $-$ )-thiogalactopyranoside (IPTG)-driven *lac* promoter. All *E. coli* strains were grown either in LB broth or on LB agar at 37 °C in aerobic conditions. Kanamycin sulfate (Fujifilm Wako Pure Chemical, Osaka, Japan) and IPTG (Fujifilm Wako Pure Chemical) were also supplemented at 50  $\mu$ g/mL and 0.01 mM, respectively, when required. To efficiently enhance the yield of MVs with extremely low endotoxin content, LB broth was supplemented with 1% glycine for the culture of EcN $\Delta$ flhD strains, because hyper-vesiculation is induced by glycine, which triggers quasi-lysis of bacterial cells through the peptidoglycan-weakened effect<sup>22,23</sup>. A laboratory serotype-14 *Streptococcus pneumoniae* strain ATCC 700676 was used in an upper respiratory infection model study. Todd Hewitt broth (30 g/L) with yeast extract (5 g/L) was used for liquid culture of *S. pneumoniae*, which was grown at 37 °C in a 5% CO<sub>2</sub> incubator. Brain heart infusion agar or Müller-Hinton II agar supplemented with 5% defibrinized blood was used for the plate culture of pneumococci, which were grown at 37 °C in an anaerobic chamber (miniMACS, Don Whitley Scientific Ltd, Shipley, UK) maintained in 80% N<sub>2</sub>, 10% H<sub>2</sub>, and 10% CO<sub>2</sub>.

#### MV isolation

The EcN $\Delta$ flhD strain and its derivatives were grown in LB broth supplemented with 1% glycine at 37 °C for 16 h under aerobic conditions. The culture supernatant was collected by centrifugation at 7190 $\times g$  for 30 min at 4 °C. The collected supernatant was filtered through a 0.22  $\mu$ m-pore PVDF membrane to eliminate contaminated cells, and subsequently ultracentrifuged at 100,000 $\times g$  for 2 h to yield MVs as sediments. MVs were resuspended in PBS (pH 7.4) and stored at -20 °C. The protein concentration of MVs was measured by Bradford assay<sup>54</sup> using bovine serum albumin (BSA) as a standard. The total protein profiles of MVs and expression of the exogenous pneumococcal CPS14 were confirmed by SDS-PAGE, followed by Coomassie brilliant blue staining and Western blot probed with rabbit polyclonal antibodies against CPS14 (#16753, Statens

Serum Institut [SSI], Hillerød, Denmark), respectively, as described previously<sup>24</sup>. CPS (SSI) was also used as an antigen. The amount of CPS14 in a single particle of CPS14<sup>+</sup>MVs was measured by quantitative dot blot, using purified CPS14 as the standard (#76943, SSI), as described previously<sup>24</sup>. The yield and particle distribution of MVs were quantified by NanoFCM (NanoFCM Inc., Xiamen, China), as described previously<sup>24</sup>. All MVs (vector control) and CPS14<sup>+</sup>MVs used in the present study were derived from the same batch.

#### Reagents and vaccines

Poly (I:C), cholera toxin B (CTB), used as antigen or adjuvant, was purchased from Merck KGaA, Darmstadt, Germany. The 13-valent pneumococcal conjugate vaccines (PCV13, Prevenar13<sup>®</sup>) and the 23-valent pneumococcal polysaccharide vaccine (PPSV23, Pneumovax23<sup>®</sup>) were purchased from Pfizer (New York, NY, USA) and Merck (Rahway, NJ, USA), respectively. PCV13 contains 13 different conjugate vaccines of serotypes 1, 3, 4, 5, 6A, 6B, 9, 14, 15B, 18C, 19A, 23F, and 33F. PPSV23 contained 23 different polysaccharide vaccines of serotypes 1, 2, 3, 4, 5, 6B, 7F, 8, 9N, 9V, 10A, 11A, 12F, 14, 15B, 17F, 18C, 19A, 19F, 20, 22F, 23F, and 33F.

#### Animal experiments

All murine experiments were reviewed and approved by the Animal Use and Care Committee of the National Institute of Infectious Diseases (NIID) (Protocol nos. 121045 and 122204) and Toho University School of Medicine (Protocol no. 21-54-386), and all protocols were performed in accordance with their institutional guidelines and regulations. All experiments except Fig. S3 were performed at NIID. The animal experiments in Fig. S3 were performed at Toho University School of Medicine. The details of each animal experiment are described in this subsection, according to the ARRIVE guidelines<sup>55</sup>. The experimental overviews are shown with the timelines of immunization, sampling, and euthanasia in Figs. 1A, 2B, 5A, 7A, 8A, S1A, S3A, and S6A. Specific pathogen-free (SPF), female BALB/c mice were purchased from Japan SLC, Inc. (Shizuoka, Japan). The polymeric immunoglobulin receptor knockout (*pIgR*<sup>-/-</sup>) and wild-type (*pIgR*<sup>+/+</sup>) mice had the BALB/c background<sup>56</sup>. The *pIgR*<sup>-/-</sup> mice were generated by mating homozygous *pIgR*<sup>+/+</sup> mice. *pIgR*<sup>-/-</sup> mice were not used for mating due to declining fertility. All mice were randomly group-housed (2–5 animals per small cage or 5–10 per large cage) with ad libitum access to water and chow diet under a standardized light cycle with 12 h on/12 h off in the animal facilities of both NIID and Toho University. Blinding was only performed in the infection experiments. In brief, the infection study was performed by a blinded observer who was not told what immunizations were given to the mice. The blinding was done after immunization by shuffling mouse groups using an Excel (Microsoft, Washington, DC, USA) randomization program.

**Immunization.** Intranasal vaccines were administered at a total volume of 10  $\mu$ L to both nostrils, i.e., 5  $\mu$ L each, under inhalation anesthesia using isoflurane at a concentration of 2.5% (Merck KGaA, Darmstadt, Germany).

Germany). The injection vaccines were subcutaneously administered at a total volume of 90  $\mu$ L to the back under inhalation anesthesia using isoflurane at a concentration of 2.5% (Merck). Details of immunization schedules are described in the figures and the figure legends.

**Sampling and preparation of whole/partial blood (serum), saliva, eye wash, nasal wash, BALF, and feces.** Whole blood was drawn at euthanasia by cardiac puncture using a 26-gauge needle syringe under inhalation anesthesia using isoflurane at a concentration of 2.5% (Merck). After coagulation, serum was recovered as the supernatant. Approximately 500  $\mu$ L serum sample was collected and stored at  $-20^{\circ}\text{C}$ . Partial blood was dropped from the tip of the tail vein cut by scissors and collected in a sampling tube for 10 min without anesthesia. After coagulation, serum was recovered as the supernatant. Approximately 50  $\mu$ L of serum sample was collected and stored at  $-20^{\circ}\text{C}$ . For saliva collection, mice were intraperitoneally injected with a secretagogue to stimulate the parasympathetic nervous system; the secretagogue was a cocktail of isoproterenol (2.0 mg/kg of body weight) (Merck) and pilocarpine (0.5 mg/kg of body weight) (Merck) in PBS, as described previously<sup>57</sup>. A few minutes after injection, saliva was secreted and collected using a pipette for 10 min without anesthesia. Approximately 100  $\mu$ L of salivary sample was collected and stored at  $-80^{\circ}\text{C}$ . Eye washes were collected from anesthetized mice by intraperitoneal injection with three ingredients in PBS: medetomidine hydrochloride, midazolam, and butorphanol tartrate, at concentrations of 0.3, 4, and 5 mg/kg of body weight, respectively, as described previously<sup>58</sup>. Mice were again injected with pilocarpine hydrochloride and isoproterenol intraperitoneally using the same method for saliva collection to stimulate the parasympathetic nervous system. Once body movement ceased, the cornea was washed with 10  $\mu$ L of PBS by pipetting 10 times without touching the pipette tip to the ocular surface and eyelid skin. Both eyes were washed with PBS twice at 15 min intervals, and eventually a total of 40  $\mu$ L eye washes from both eyes ( $2 \times 10 \mu\text{L}$  per eye) were pooled and stored at  $-20^{\circ}\text{C}$ . Fresh feces obtained from mice were suspended in PBS at a concentration of 100 mg of feces/mL in the sample tubes. After vortexing the tubes for 5 min and centrifuging at  $17,400 \times g$  for 5 min, the clear supernatant was collected as a fecal suspension and stored at  $-20^{\circ}\text{C}$ . After euthanasia, nasal wash and BALF samples were collected. Nasal wash samples were obtained by washing the nasal cavities of the isolated upper heads three times with 200  $\mu$ L/wash of PBS containing 0.1% BSA. In total, 600  $\mu$ L of nasal wash samples were pooled and stored at  $-20^{\circ}\text{C}$ . BALF samples were obtained by washing the en bloc dissected lung with trachea with 2 mL of PBS. The washing procedure was repeated once more using the initial wash solution. The BALF samples were stored at  $-20^{\circ}\text{C}$ .

**Upper respiratory tract infection model.** In the continuation of the long-term animal experiment described in (a) (Fig. 1B), the upper respiratory infection study was performed in SPF animal facilities at NIID and Toho University that fulfilled animal biosafety level 2 (BSL2). In preliminary experiments to determine a suitable time point for nasal wash sampling (Fig. S3), 1 day (24 h), 3 days, or 7 days after the pathogen inoculation, serum and nasal wash were collected from the mice. In total, 40 mice were subjected to the bacterial clearance assay (Fig. 7) at the end of the long-term experiments. Because the number of mice was too large to assay all at once, the mice ( $n = 40$ ) were divided into Class I and Class II, which were assayed at weeks 56 and 59, respectively. Eighteen mice were allocated to Class I: Grp. A ( $n = 3$ ), Grp. B ( $n = 3$ ), Grp. C ( $n = 3$ ), Grp. D ( $n = 3$ ), Grp. E ( $n = 3$ ), and Grp. F ( $n = 3$ ). Twenty-two mice were allocated to Class II: Grp. A ( $n = 5$ ), Grp. B ( $n = 4$ ), Grp. C ( $n = 5$ ), Grp. D ( $n = 5$ ), and Grp. E ( $n = 3$ ). The timeline of the infection experiment is shown in Fig. 7A. The 62- or 65-week-old female BALB/c mice (Japan SLC, Inc, Hamamatsu, Japan) were anesthetized by intraperitoneal injection with three ingredients in PBS: medetomidine hydrochloride, midazolam, and butorphanol tartrate, at concentrations of 0.3, 4, and 5 mg/kg of body weight, respectively<sup>58</sup>, prior to infection. Anesthetized

mice were intranasally administered with  $2 \times 10^5$  CFU of serotype 14 pneumococcal strain ATCC 700676 in 10  $\mu$ L of PBS. Twenty-four hours after pathogen inoculation, samples of serum, nasal wash, and BALF were collected from mice. The CPS14-specific antibodies in all samples were examined by ELISA. Pneumococcal clearance in the upper respiratory tract was examined by both real-time PCR and CFU counting in the nasal wash. Bacterial leakage to the lower respiratory tract was confirmed by CFU counting using BALF samples of all the mice used for the upper respiratory tract infection experiments. Data obtained from real-time PCR assays were well-correlated with those of the CFU counting method (Fig. S5). However, the detection sensitivity of the real-time PCR assay was better than that of CFU counting (Fig. S4). The discrepancy is probably because the real-time PCR-based assay does not assess viable bacterial numbers, but can detect the amount of bacterial DNA.

**Upper respiratory tract infection model using polymeric immunoglobulin receptor knock-out mice.** Six- to 8-week-old female *pIgR*<sup>+/+</sup> and *pIgR*<sup>-/-</sup> mice were used for upper respiratory tract infection experiments (Fig. 8). The *pIgR*<sup>+/+</sup> and *pIgR*<sup>-/-</sup> mice were intranasally immunized three times with MVs (vector control) or CPS14<sup>+</sup>MVs (0.013  $\mu$ g, CPS14 equivalent) at 3-week intervals. Those mice were intranasally inoculated with  $2 \times 10^5$  CFU of strain ATCC 700676. Twenty-four hours after infection, pneumococcal colonization at the upper respiratory tract was evaluated by CFU counting and real-time PCR in nasal wash samples. See the details in the “Bacterial clearance assay” section.

## ELISA

**CPS14-coating ELISA.** The amounts of CPS14-specific antibodies in serum, saliva, nasal wash, BALF, eye wash, and fecal samples from mice were examined by ELISA, as described previously<sup>24</sup> with some modifications. CPS14 antigen was coated onto ELISA plates at 125 ng per well (#675061, Grainer Bio-One GmbH, Frickenhausen, Germany). Alkaline phosphatase (AP)-labeled anti-mouse IgG Fcγ fragment was purchased from Jackson ImmunoResearch (#315-055-008, West Grove, PA, USA), and used at 1:1000 dilution. AP-labeled anti-mouse IgM, IgE, IgA, IgG1, IgG2a, IgG2b, IgG3 were purchased from Southern Biotech (Birmingham, AL, USA), and used at 1:1000 dilutions. Regarding CPS14-specific serum IgG1 and IgG2a, the endpoint titers were also expressed as the reciprocal  $\log_2$  of the last dilution that provided an  $\text{OD}_{405}$  of 0.05 greater than the background level, which was determined as the average of 2 mice immunized with PBS (mock immunization) in the same ELISA plate. Chromogenic development using para-nitrophenyl phosphate was recorded as absorbance at 405 nm at 15, 30, 60, 120 min with a Cytation5 (Biotek, Winooski, VT, USA) plate reader. All  $\text{OD}_{405}$  values were subtracted from the average value of three wells incubated in the same plate with PBS without any mouse sample.

**MV-coating ELISA.** The amounts of MV-specific serum IgG and nasal wash IgA were examined by ELISA, as described previously<sup>59</sup> with some modifications. MVs isolated from culture supernatant of *EcNΔflhD/pWSK129* (vector control) were coated onto ELISA plates at 100 ng/well. Except for antigen coating, ELISA was performed in the same manner as described in the subsection of “CPS14-coating ELISA”.

## Bacterial clearance assay

The nasal wash or BALF samples were 10-fold serially diluted and inoculated onto Müller–Hinton II agar plates (Becton, Dickinson [BD] & Co., Sparks, MD, USA) supplemented with 5% defibrinated sheep blood. The plates were subsequently incubated at  $37^{\circ}\text{C}$  in an anaerobic chamber (miniMACS anaerobic workstation, Don Whitley Scientific Ltd.) using 80%  $\text{N}_2$ , 10%  $\text{H}_2$ , and 10%  $\text{CO}_2$ . After 24 h of incubation, the colony numbers on the plate were enumerated. The nasal wash samples were also subjected to *S. pneumoniae*-specific real-time PCR by detecting the pneumococcal autolysin gene, *lytA*. The *lytA* copy numbers in 2  $\mu$ L of the 600  $\mu$ L of nasal wash

samples were quantified. The total copy numbers in the nasal cavity were estimated by the following formula: (*lytA* copy numbers/2  $\mu$ L)  $\times$  300  $\mu$ L. TaqMan probe-based real-time PCR was performed using an Applied Biosystems 7500 Fast Real-Time PCR System (Thermo Fisher Scientific, Waltham, MA, USA) with Premix Ex Taq Probe qPCR (Takara Bio, Shiga, Japan). The sequences of the forward primer, the reverse primer, and the probe were 5'-CGACTGAAATGTCAGTAGGAGAAGAT-3', 5'-AATA-CAGTCCATCAATTACTGCAATACTC-3', [FAM]5'-TGTCAATTGCTTGCCTAACTTGATGGTCTC-3'[TAMRA], respectively. The baseline values of CFU and real-time PCR (*lytA* copy number) in the nasal cavity of *pIgR*<sup>+/+</sup> and *pIgR*<sup>-/-</sup> mice that indicated pneumococcal colonization 24 h after challenge were approximately one order lower than those in the case of BALB/c mice purchased from Japan SLC Inc. The reason the level of colonization in the nasal cavity differs among them remains unknown; however, the discrepancy may be due to the differences in genetic backgrounds or environmental factors during breeding.

### Opsonophagocytic killing assay (OPA)

OPA measures the ability of antibodies to mediate phagocytic killing, usually in the presence of complement. In the case of pneumococcal vaccines, measurement of functional antibody responses in OPA may correlate with clinical protection more closely than ELISA antibody levels<sup>60,61</sup>. The opsonic activities of serum samples collected from 62- or 65-week-old mice were measured against pneumococcal serotype 14 (STREP14, BEI Resources Catalog No. NR-13396)<sup>62</sup> by the opsonophagocytic killing assay. The opsonophagocytic killing assay was conducted following the pneumococcal antibody opsonization assay protocol (UAB-MOPA) provided by the WHO pneumococcal reference laboratory ([www.vaccine.uab.edu](http://www.vaccine.uab.edu))<sup>63,64</sup>. All mouse serum samples were inactivated, and this experiment was performed with the serum samples at an initial 4-fold dilution. Opsonic index (OI) values were calculated using the Opsotiter 3 software (provided by the WHO pneumococcal reference laboratory). OI values were calculated as the reciprocal of the serum dilution that killed 50% of the test bacteria<sup>64</sup>.

### Statistical analysis

Statistical analysis was performed with a Mann–Whitney *U* test or Kruskal–Wallis test. *P* values  $< 0.05$  were considered to indicate statistical significance.

### Data availability

All data are presented in the main text or the supplementary materials and are available upon reasonable request from the corresponding author, Ryoma Nakao, by e-mail (ryoma73@niid.go.jp).

Received: 19 May 2025; Accepted: 4 December 2025;

Published online: 23 December 2025

### References

1. Collaborators, G. B. D. A. R Global mortality associated with 33 bacterial pathogens in 2019: a systematic analysis for the Global Burden of Disease Study 2019. *Lancet* **400**, 2221–2248 (2022).
2. Shi, T. et al. Global and regional burden of hospital admissions for pneumonia in older adults: a systematic review and meta-analysis. *J. Infect. Dis.* **222**, S570–S576 (2020).
3. LeBlanc, J. J. et al. Burden of vaccine-preventable pneumococcal disease in hospitalized adults: a Canadian Immunization Research Network (CIRN) Serious Outcomes Surveillance (SOS) network study. *Vaccine* **35**, 3647–3654 (2017).
4. Yu, J. et al. New pneumococcal serotype 20C is a WciG O-acetyltransferase deficient variant of canonical serotype 20B. *Microbiol. Spectr.* **13**, e0244324 (2025).
5. Ganaie, F. et al. A new pneumococcal capsule type, 10D, is the 100th serotype and has a large cps fragment from an oral *Streptococcus*. *mBio* **11**, <https://doi.org/10.1128/mBio.00937-20> (2020).
6. Ganaie, F. A. et al. Discovery and characterization of pneumococcal serogroup 36 capsule subtypes, serotypes 36A and 36B. *J. Clin. Microbiol.* **61**, e0002423 (2023).
7. Collaborators, G. B. D. L. R. I Estimates of the global, regional, and national morbidity, mortality, and aetiologies of lower respiratory infections in 195 countries, 1990–2016: a systematic analysis for the Global Burden of Disease Study 2016. *Lancet Infect. Dis.* **18**, 1191–1210 (2018).
8. Kalizang’oma, A. et al. Clonal expansion of a *Streptococcus pneumoniae* serotype 3 capsule variant sequence type 700 with enhanced vaccine escape potential after 13-valent pneumococcal conjugate vaccine introduction. *J. Infect. Dis.* **230**, e189–e198 (2024).
9. Candeias, C. et al. *Streptococcus pneumoniae* carriage, serotypes, genotypes, and antimicrobial resistance trends among children in Portugal, after introduction of PCV13 in National Immunization Program: a cross-sectional study. *Vaccine* **42**, 126219 (2024).
10. von Mollendorf, C. & Ong-Lim, A. L. T. How have pneumococcal conjugate vaccines changed the pneumococcal disease landscape?. *Lancet Infect. Dis.* **25**, 367–369 (2025).
11. Ranjbar, R. & Alam, M. Antimicrobial Resistance Collaborators (2022). Global burden of bacterial antimicrobial resistance in 2019: a systematic analysis. *Evid. Based Nurs.* <https://doi.org/10.1136/ebnurs-2022-103540> (2023).
12. Hyams, C. et al. Serotype distribution and disease severity in adults hospitalized with *Streptococcus pneumoniae* infection, Bristol and Bath, UK, 2006–2022. *Emerg. Infect. Dis.* **29**, 1953–1964 (2023).
13. Li, L. et al. Epidemiological characteristics and antibiotic resistance mechanisms of *Streptococcus pneumoniae*: an updated review. *Microbiol. Res.* **266**, 127221 (2023).
14. Kobayashi, M. et al. Use of 21-valent pneumococcal conjugate vaccine among U.S. adults: recommendations of the Advisory Committee on Immunization Practices—United States, 2024. *MMWR Morb. Mortal Wkly Rep.* **73**, 793–798 (2024).
15. Rappuoli, R. Glycoconjugate vaccines: principles and mechanisms. *Sci. Transl. Med.* **10**, <https://doi.org/10.1126/scitranslmed.aat4615> (2018).
16. Chen, C. et al. Effect and cost-effectiveness of pneumococcal conjugate vaccination: a global modelling analysis. *Lancet Glob. Health* **7**, e58–e67 (2019).
17. Belshe, R. B. et al. Safety, efficacy, and effectiveness of live, attenuated, cold-adapted influenza vaccine in an indicated population aged 5–49 years. *Clin. Infect. Dis.* **39**, 920–927 (2004).
18. Eiden, J. et al. Intranasal M2SR (M2-deficient single replication) H3N2 influenza vaccine provides enhanced mucosal and serum antibodies in adults. *J. Infect. Dis.* **227**, 103–112 (2022).
19. Babu, T. M., Jackson, L. A. & El Sahly, H. M. Next-generation SARS-CoV-2 vaccine formulations and alternative routes of administration. *J. Infect. Dis.* **231**, 44–48 (2025).
20. Chu, K. et al. A randomized phase I trial of intranasal SARS-CoV-2 vaccine dNS1-RBD in children aged 3–17 years. *NPJ Vaccines* **10**, 50 (2025).
21. Li, J. X. et al. Safety and immunogenicity of heterologous boost immunisation with an orally administered aerosolised Ad5-nCoV after two-dose priming with an inactivated SARS-CoV-2 vaccine in Chinese adults: a randomised, open-label, single-centre trial. *Lancet Respir. Med.* **10**, 739–748 (2022).
22. Hirayama, S. & Nakao, R. Glycine induction method: effective production of immunoactive bacterial membrane vesicles with low endotoxin content. *Methods Mol. Biol.* **2414**, 207–226 (2022).
23. Hirayama, S. & Nakao, R. Glycine significantly enhances bacterial membrane vesicle production: a powerful approach for isolation of LPS-reduced membrane vesicles of probiotic *Escherichia coli*. *Microb. Biotechnol.* **13**, 1162–1178 (2020).

24. Nakao, R. et al. A highly immunogenic vaccine platform against encapsulated pathogens using chimeric probiotic *Escherichia coli* membrane vesicles. *NPJ Vaccines* **7**, 153 (2022).
25. Musher, D. M. et al. Safety and antibody response, including antibody persistence for 5 years, after primary vaccination or revaccination with pneumococcal polysaccharide vaccine in middle-aged and older adults. *J. Infect. Dis.* **201**, 516–524 (2010).
26. van Werkhoven, C. H., Huijts, S. M., Bolkenbaas, M., Grobbee, D. E. & Bonten, M. J. The impact of age on the efficacy of 13-valent pneumococcal conjugate vaccine in elderly. *Clin. Infect. Dis.* **61**, 1835–1838 (2015).
27. Thevarajan, N. et al. *Streptococcus pneumoniae* colonization disrupts the microbial community within the upper respiratory tract of aging mice. *Infect. Immun.* **84**, 906–916 (2016).
28. Cubas, R. et al. Virus-like particle (VLP) lymphatic trafficking and immune response generation after immunization by different routes. *J. Immunother.* **32**, 118–128 (2009).
29. Reddy, S. T. et al. Exploiting lymphatic transport and complement activation in nanoparticle vaccines. *Nat. Biotechnol.* **25**, 1159–1164 (2007).
30. Wilson, J. T. A sweeter approach to vaccine design. *Science* **363**, 584–585 (2019).
31. Munoz-Wolf, N. et al. Non-canonical inflammasome activation mediates the adjuvanticity of nanoparticles. *Cell Rep. Med.* **4**, 100899 (2023).
32. Degn, S. E. & Tolar, P. Towards a unifying model for B-cell receptor triggering. *Nat. Rev. Immunol.* **25**, 77–91 (2025).
33. Tolar, P. & Pierce, S. K. Unveiling the B cell receptor structure. *Science* **377**, 819–820 (2022).
34. Olivo-Martinez, Y. et al. Modulation of serotonin-related genes by extracellular vesicles of the probiotic *Escherichia coli* Nissle 1917 in the interleukin-1beta-induced inflammation model of intestinal epithelial cells. *Int. J. Mol. Sci.* **25**, <https://doi.org/10.3390/ijms25105338> (2024).
35. Canas, M. A., Fabrega, M. J., Gimenez, R., Badia, J. & Baldoma, L. Outer membrane vesicles from probiotic and commensal *Escherichia coli* activate NOD1-mediated immune responses in intestinal epithelial cells. *Front. Microbiol.* **9**, 498 (2018).
36. Jerving, S. The long road ahead for COVID-19 vaccination in Africa. *Lancet* **398**, 827–828 (2021).
37. Loyo, E. S. L., Gonzalez, M. J. & Esparza, J. Venezuela is collapsing without COVID-19 vaccines. *Lancet* **397**, 1806 (2021).
38. Li, X. et al. Estimating the health impact of vaccination against ten pathogens in 98 low-income and middle-income countries from 2000 to 2030: a modelling study. *Lancet* **397**, 398–408 (2021).
39. Zhang, J. R. et al. The polymeric immunoglobulin receptor translocates pneumococci across human nasopharyngeal epithelial cells. *Cell* **102**, 827–837 (2000).
40. Briles, D. E. et al. PspA and PspC: their potential for use as pneumococcal vaccines. *Microb. Drug Resist.* **3**, 401–408 (1997).
41. Hammerschmidt, S., Talay, S. R., Brandtzaeg, P. & Chhatwal, G. S. SpsA, a novel pneumococcal surface protein with specific binding to secretory immunoglobulin A and secretory component. *Mol. Microbiol.* **25**, 1113–1124 (1997).
42. Lu, L., Lamm, M. E., Li, H., Corthesy, B. & Zhang, J. R. The human polymeric immunoglobulin receptor binds to *Streptococcus pneumoniae* via domains 3 and 4. *J. Biol. Chem.* **278**, 48178–48187 (2003).
43. Iovino, F. et al. Pneumococcal meningitis is promoted by single cocci expressing pilus adhesin RrgA. *J. Clin. Investig.* **126**, 2821–2826 (2016).
44. Iovino, F. et al. plgR and PECAM-1 bind to pneumococcal adhesins RrgA and PspC mediating bacterial brain invasion. *J. Exp. Med.* **214**, 1619–1630 (2017).
45. Renegar, K. B., Small, P. A. Jr, Boykins, L. G. & Wright, P. F. Role of IgA versus IgG in the control of influenza viral infection in the murine respiratory tract. *J. Immunol.* **173**, 1978–1986 (2004).
46. Renegar, K. B., Jackson, G. D. & Mestecky, J. In vitro comparison of the biologic activities of monoclonal monomeric IgA, polymeric IgA, and secretory IgA. *J. Immunol.* **160**, 1219–1223 (1998).
47. Suzuki, T. et al. Relationship of the quaternary structure of human secretory IgA to neutralization of influenza virus. *Proc. Natl. Acad. Sci. USA* **112**, 7809–7814 (2015).
48. Saito, S. et al. IgA tetramerization improves target breadth but not peak potency of functionality of anti-influenza virus broadly neutralizing antibody. *PLoS Pathog.* **15**, e1007427 (2019).
49. Keller, L. E., Robinson, D. A. & McDaniel, L. S. Nonencapsulated *Streptococcus pneumoniae*: emergence and pathogenesis. *mBio* **7**, e01792 (2016).
50. Nissle, A. Über die Grundlagen einer neuen ursächlichen Bekämpfung der pathologischen Darmflora. *Dtsch. Med. Wochenschr.* **42**, 1181–1184 (1916).
51. Wang, R. F. & Kushner, S. R. Construction of versatile low-copy-number vectors for cloning, sequencing and gene expression in *Escherichia coli*. *Gene* **100**, 195–199 (1991).
52. Price, N. L. et al. Glycoengineered outer membrane vesicles: a novel platform for bacterial vaccines. *Sci. Rep.* **6**, 24931 (2016).
53. Imohl, M., Reinert, R. R., Ocklenburg, C. & van der Linden, M. Association of serotypes of *Streptococcus pneumoniae* with age in invasive pneumococcal disease. *J. Clin. Microbiol.* **48**, 1291–1296 (2010).
54. Bradford, M. M. A rapid and sensitive method for the quantitation of microgram quantities of protein utilizing the principle of protein-dye binding. *Anal. Biochem.* **72**, 248–254 (1976).
55. Percie du Sert, N. et al. The ARRIVE guidelines 2.0: updated guidelines for reporting animal research. *PLoS Biol.* **18**, e3000410 (2020).
56. Asahi, Y. et al. Protection against influenza virus infection in polymeric Ig receptor knockout mice immunized intranasally with adjuvant-combined vaccines. *J. Immunol.* **168**, 2930–2938 (2002).
57. Abdus Salam, M. et al. Establishment of an animal model using recombinant NOD.B10.D2 mice to study initial adhesion of oral streptococci. *Clin. Diagn. Lab. Immunol.* **11**, 379–386 (2004).
58. Kawai, S., Takagi, Y., Kaneko, S. & Kurosawa, T. Effect of three types of mixed anesthetic agents alternate to ketamine in mice. *Exp. Anim.* **60**, 481–487 (2011).
59. Bai, D., Nakao, R., Ito, A., Uematsu, H. & Senpuku, H. Immunoreactive antigens recognized in serum samples from mice intranasally immunized with *Porphyromonas gingivalis* outer membrane vesicles. *Pathog. Dis.* **73**, <https://doi.org/10.1093/femspd/ftu006> (2015).
60. Henckaerts, I., Durant, N., De Grave, D., Schuerman, L. & Poolman, J. Validation of a routine opsonophagocytosis assay to predict invasive pneumococcal disease efficacy of conjugate vaccine in children. *Vaccine* **25**, 2518–2527 (2007).
61. Romero-Steiner, S. et al. Use of opsonophagocytosis for serological evaluation of pneumococcal vaccines. *Clin. Vaccine Immunol.* **13**, 165–169 (2006).
62. Kim, K. H., Yu, J. & Nahm, M. H. Efficiency of a pneumococcal opsonophagocytic killing assay improved by multiplexing and by coloring colonies. *Clin. Diagn. Lab. Immunol.* **10**, 616–621 (2003).
63. Burton, R. L. & Nahm, M. H. Development and validation of a fourfold multiplexed opsonization assay (MOPA4) for pneumococcal antibodies. *Clin. Vaccine Immunol.* **13**, 1004–1009 (2006).
64. Nahm, M. H. & Burton, R. L. Protocol for multiplexed opsonophagocytic killing assay (UAB-MOPA) for antibodies against *Streptococcus pneumoniae* Protoc. UAB-MOPA 1–43 Version E.02, <https://www.vaccine.uab.edu/index.html> (2014).

## Acknowledgements

We thank Yuriko Tanaka (Osaka University, Japan), Fumiko Takashima (JIHS, Japan), Junko Sugita (JIHS), Naomi Nojiri (JIHS), Izuho Suwa (JIHS), Hiroki Uchiyama (JIHS), Ryunosuke Tominaga (JIHS), Aoi Takahashi (JIHS), Yusuke Iwabuchi (JIHS) for their technical support. We thank Saeko Morino

(JIHS), Motoi Suzuki (JIHS), Bin Chang (JIHS), Michinaga Ogawa (JIHS), Satoru Hirayama (Niigata University, Japan), and Hidenobu Senpuku (Nihon University, Japan) for the fruitful discussion regarding the present study. We thank Bernt Eric Uhlin (Umeå University, Sweden), Mario F. Feldman (Washington University, USA), M. Florencia Haurat (Washington University), Satoshi Matsumoto (Yakurt Central Institute, Japan), and Masanobu Nanno (Yakurt Central Institute) for providing biological materials. Japan Society for the Promotion of Science (KAKENHI) 20H03861 (R.N.), Japan Society for the Promotion of Science (KAKENHI) 21KK0164 (R.N.), Japan Society for the Promotion of Science (KAKENHI) 21K18284 (R.N.), Japan Society for the Promotion of Science (KAKENHI) 22K08609 (S.K.), Mitsui Sumitomo Insurance Welfare Foundation Research Grant 2021 (S.K.).

### Author contributions

R.N. designed the study, wrote the first draft of the manuscript, and did the final edits. R.N., S.K., E.K., S.H., and Y.O. conducted experiments. R.N., S.K., K.A., T.Y., E.K., S.H., K.T., Y.O., N.N., M.O., and Y.A. reviewed the manuscript. All authors contributed to the article and approved the submitted version.

### Competing interests

The authors declare no competing interests.

### Additional information

**Supplementary information** The online version contains supplementary material available at <https://doi.org/10.1038/s41541-025-01345-0>.

**Correspondence** and requests for materials should be addressed to Ryoma Nakao.

**Reprints and permissions information** is available at <http://www.nature.com/reprints>

**Publisher's note** Springer Nature remains neutral with regard to jurisdictional claims in published maps and institutional affiliations.

**Open Access** This article is licensed under a Creative Commons Attribution-NonCommercial-NoDerivatives 4.0 International License, which permits any non-commercial use, sharing, distribution and reproduction in any medium or format, as long as you give appropriate credit to the original author(s) and the source, provide a link to the Creative Commons licence, and indicate if you modified the licensed material. You do not have permission under this licence to share adapted material derived from this article or parts of it. The images or other third party material in this article are included in the article's Creative Commons licence, unless indicated otherwise in a credit line to the material. If material is not included in the article's Creative Commons licence and your intended use is not permitted by statutory regulation or exceeds the permitted use, you will need to obtain permission directly from the copyright holder. To view a copy of this licence, visit <http://creativecommons.org/licenses/by-nc-nd/4.0/>.

© The Author(s) 2025